Molecular Biology of the Cell
Vol. 21, 3552–3566, October 15, 2010

α-Arrestins Aly1 and Aly2 Regulate Intracellular Trafficking in Response to Nutrient Signaling

Allyson F. O'Donnell,* Alex Apffel,† Richard G. Gardner,‡ and Martha S. Cyert*

*Department of Biology, Stanford University, Stanford, CA 94305-5020; †Agilent Laboratories, Santa Clara, CA 95051; and ‡Department of Pharmacology, University of Washington, Seattle, WA 98195-7280

Submitted July 27, 2010; Revised August 6, 2010; Accepted August 12, 2010
Monitoring Editor: David G. Drubin

Extracellular signals regulate trafficking events to reorganize proteins at the plasma membrane (PM); however, few effectors of this regulation have been identified. β-Arrestins relay signaling cues to the trafficking machinery by controlling agonist-stimulated endocytosis of G-protein–coupled receptors. In contrast, we show that yeast α-arrestins, Aly1 and Aly2, control intracellular sorting of Gap1, the general amino acid permease, in response to nutrients. These studies are the first to demonstrate association of α-arrestins with clathrin and clathrin adaptor proteins (AP) and show that Aly1 and Aly2 interact directly with the γ-subunit of AP-1, Apl4. Aly2-dependent trafficking of Gap1 requires AP-1, which mediates endosome-to-Golgi transport, and the nutrient-regulated kinase, Npr1, which phosphorylates Aly2. During nitrogen starvation, Npr1 phosphorylation of Aly2 may stimulate Gap1 incorporation into AP-1/clathrin-coated vesicles to promote Gap1 trafficking from endosomes to the *trans*-Golgi network. Ultimately, increased Aly1-/Aly2-mediated recycling of Gap1 from endosomes results in higher Gap1 levels within cells and at the PM by diverting Gap away from trafficking pathways that lead to vacuolar degradation. This work defines a new role for arrestins in membrane trafficking and offers insight into how α-arrestins coordinate signaling events with protein trafficking.

INTRODUCTION

Cell surface proteins are rapidly reorganized to ensure optimal nutrient uptake in response to environmental changes. To accomplish this, cells coordinately regulate opposing plasma membrane (PM) processes: endocytosis of existing proteins and delivery of new proteins. In response to nitrogen starvation, yeast cells make a critical switch; Tat2, a tryptophan-specific permease, is endocytosed and degraded, whereas Gap1, the general amino acid permease, is delivered to the PM (Schmidt *et al.*, 1998; De Craene *et al.*, 2001). These fundamentally similar processes require the formation of transport vesicles bearing specific membrane cargos and delivery of those vesicles to distinct cellular locations. The trafficking machinery that generates vesicles and restricts vesicle fusion to appropriate target compartments is well described (Bonifacino and Lippincott-Schwartz, 2003; Ungar and Hughson, 2003). In contrast, little is known about how extracellular signals drive specific trafficking events in cells.

Arrestins are critical adaptors that direct trafficking of specific cargos in response to extracellular signals. Arrestin family members contain conserved N- and C-terminal arrestin-fold domains, but can be divided into α- and β-arrestin classes based on primary sequence and structural features (Alvarez, 2008). β-Arrestins, a small, recently evolved branch of the family (Alvarez, 2008), couple agonist-induced signaling to the endocytosis of G-protein–coupled receptors (GPCRs), a large class of receptors that regulate a vast array of biological processes (Shenoy and Lefkowitz, 2003). Agonists stimulate GPCR signaling and induce receptor phosphorylation (Krupnick and Benovic, 1998). β-Arrestins bind phosphorylated GPCRs and promote endocytosis by recruiting a ubiquitin ligase that ubiquitinates the receptor and β-arrestin (Shenoy *et al.*, 2001) and by interacting with vesicle coat proteins, such as clathrin and clathrin adaptor complex 2 (AP-2; Goodman *et al.*, 1996; Laporte *et al.*, 1999). The postendocytic β-arrestin–GPCR interaction determines if the receptor recycles to the PM, is degraded in the lysosome, or forms an endosomal signaling complex (Shenoy and Lefkowitz, 2003). Thus, β-arrestins respond to signaling cues and regulate the trafficking of select cargos by direct interaction with vesicle coat proteins.

In comparison to β-arrestins, the widely conserved, ancestral α-arrestins are not well studied; only one of the six mammalian α-arrestins has an ascribed trafficking function. Most α-arrestins in *Saccharomyces cerevisiae* interact with and are ubiquitinated by the Rsp5 ubiquitin ligase (Kee *et al.*, 2006; Gupta *et al.*, 2007; Lin *et al.*, 2008). Several of these proteins regulate the endocytosis, and in some cases Rsp5-dependent ubiquitination, of specific membrane transporters (Lin *et al.*, 2008; Nikko *et al.*, 2008; Nikko and Pelham, 2009). However, it is not clear if all α-arrestins regulate endocytosis, as systematic screens with four membrane transporters failed to identify endocytic activ-

This article was published online ahead of print in *MBoC in Press* (http://www.molbiolcell.org/cgi/doi/10.1091/mbc.E10–07–0636) on August 25, 2010.

Address correspondence to: Martha S. Cyert (mcyert@stanford.edu).

Abbreviations used: ALY, arrestin-like yeast protein; AP-1, adaptor protein complex 1; AP-2, adaptor protein complex 2; AzC, azetidine 2-carboxylic acid; CArr, C-terminal arrestin-fold; E/H, adaptin ear/hinge domain; MIN, minimal medium; MVB, multivesicular body; NArr, N-terminal arrestin-fold; NH_4, ammonium; PM, plasma membrane; SC, synthetic complete medium; TGN, *trans*-Golgi network; WB, Western blot.

ity for certain family members, including Aly1 and Aly2, closely related α-arrestins that are the focus of these studies (Nikko and Pelham, 2009).

Here we show that, in striking contrast to the endocytic function of other arrestins, Aly1 and Aly2, (arrestin-like yeast proteins) regulate intracellular trafficking of Gap1. Importantly, Aly1 and Aly2 copurify with clathrin and clathrin-adaptor protein (AP) complexes in vivo and interact directly with the γ-subunit of AP-1 in vitro, suggesting that, like their β-arrestin relatives, α-arrestins promote cargo incorporation into clathrin-coated vesicles (CCVs). Nutrient signaling regulates both Aly1- and Aly2-mediated trafficking. Aly2 requires Npr1, a TORC1- and nutrient-regulated kinase that stimulates Gap1 trafficking to the PM through an unknown mechanism (De Craene *et al.*, 2001), to increase Gap1 levels in intracellular compartments and at the PM. Npr1 interacts with and phosphorylates Aly2 and may directly regulate Aly2 function. Thus, these studies identify signaling and vesicle coat proteins required for α-arrestin–mediated intracellular trafficking.

MATERIALS AND METHODS

Growth Media and General Methods

Synthetic complete medium (SC) was prepared as described for YNB medium in (Johnston *et al.*, 1977) with the addition of 2.5 g/l ammonium (NH_4) sulfate, 40 μg/ml amino acids, and 20 μg/ml nucleoside bases. The same formulation lacking amino acids/nucleoside bases was used for minimal medium (MIN); required supplements were added to MIN to support growth of auxotrophic strains. Alternative nitrogen sources were used as indicated.

Cells used in phenotype analyses on plates were grown to saturation and then plated in fivefold serial dilutions with a starting concentration of 1.0×10^7 cells. Plates were grown at 30°C for the time indicated in each panel. YEPD media is described in Hartwell (1967).

Plasmids were transformed into yeast using the lithium-acetate method (Ausubel, 1991).

Yeast Strains

Yeast strains used in this study are described in Table S1. Details of specific strain constructions generated for this study are as follows: *aly1*Δ *aly2*Δ double mutant cells were constructed using two different approaches. First, strain 5092 (*MAT***a** *aly1*Δ::*KanMX4*) was mated to strain 11339 (*MATα aly2*Δ::*KanMX4*), the resulting diploids were sporulated and nonparental ditype (NPD) tetrads selected. Appropriate segregation was monitored for four different marker loci to verify NPD tetrads. In this way spores D2–6A, D2–4C and D12–6B were obtained, all of which carry the *aly1*Δ::*KanMX4 aly2*Δ::*KanMX4* but with a variety of additional auxotrophies and mating types (see Supplemental Table S1). Growth of *aly1*Δ *aly2*Δ spores were assayed in the presence of NaCl, LiCl, MgCl, KCl, calcofluor white, congo red, caffeine, rapamycin, and alternative carbon sources (i.e., glycerol, ethanol, sucrose, raffinose, galactose, and maltose), and all grew equivalently (data not shown).

The second approach to generating *aly1*Δ *aly2*Δ was to make consecutive gene deletions in Y2454 cells. The p314-ALY1KO plasmid was digested with ClaI/NotI and the *Nat*MX4 cassette flanked by sequence up- and downstream of the *ALY1* coding region was transformed as per (Goldstein and McCusker, 1999) into Y2454 cells. Nat-resistant colonies were selected and integration site verified by PCR. Similarly, p314-ALY2KO plasmid was digested with KpnI/SpeI, and the *URA3* gene flanked by sequence up- and down-stream of the *ALY2* coding region was transformed into Y2454 cells, and uracil prototrophs were selected. Replacement of the chromosomal *ALY2* coding sequence with *URA3* was verified by PCR. To generate the *aly1*Δ *aly2*Δ mutant, the *aly1*Δ::*NatMX4* strain was used in a second knockout transformation with the KpnI/SpeI fragment of p314-ALY2KO. Phenotypes observed for *aly1*Δ::*NatMX4 aly2*Δ::*URA3* strain generated in Y2454 cells were consistent with those seen for the *aly1*Δ::*KanMX4 aly2*Δ::*KanMX4* in the BY4741 background (data not shown).

Prototrophic, homozygous diploid *aly1*ΔΔ *aly2*ΔΔ cells were obtained by mating D12–6B with D2–4C that had been transformed with pCK230 and selecting for diploids on SC-Ura$^-$Lys$^-$Met$^-$ medium. Diploids were then transformed with pRS313 and either pRS425, pRS425-Aly1, or pRS425-Aly2.

The *bul1*Δ *bul2*Δ *aly1*Δ *aly2*Δ strain was obtained by crossing *aly1*Δ::*NatMX4 aly2*Δ::*URA3* with *bul1*Δ *bul2*Δ spore 3D (which was generated by mating and sporulating strains 861 and 16511 and selecting NPD tetrads). Sporulation of the resulting diploid gave rise to two quadruple mutants, *bul1*Δ *bul2*Δ *aly1*Δ *aly2*Δ spores 7D and 20A, which displayed equivalent sensitivities to azetidine 2-carboxylic acid (AzC) in growth assays.

The *vps4*Δ *aly1*Δ *aly2*Δ strain was obtained by crossing *aly1*Δ::*NatMX4 aly2*Δ::*URA3* with strain 5588 containing *vps4*Δ::*KanMX4*. Sporulation of the resulting diploid gave two *vps4*Δ::*KanMX4 aly1*Δ::*NatMX4 aly2*Δ::*URA3* triple mutant spores that exhibited identical sensitivities in growth assays, including sensitivity to AzC.

The *chs6*Δ *aly1*Δ *aly2*Δ strain was obtained by crossing *aly1*Δ::*NatMX4 aly2*Δ::*URA3* with strain 1324 containing *chs6*Δ::*KanMX4*. Sporulation of the resulting diploid gave two *chs6*Δ::*KanMX4 aly1*Δ::*NatMX4 aly2*Δ::*URA3* triple mutant spores and both were examined in the CFW bud scar-staining assay. Similarly, the *chs6*Δ *apl2*Δ strain was obtained by crossing cells from strain 1324 to a *MATα apl2*Δ::*KanMX4* generated by sporulating the homozygous diploid deletion strain 34985. NPD tetrad products were selected from sporulation of this diploid, and proper segregation of four independent loci was monitored to confirm NPD tetrads. As expected, both of the *chs6*Δ::*KanMX4 apl2*Δ::*KanMX4* spores (9A and 9B) alleviated the bud scar defect in a *chs6*Δ::*KanMX4* cells.

The BJ5459-Npr1-MYC strain contains a chromosomally integrated Npr1–13xMyc marked with the KanMX6 cassette. The PCR product obtained from using the pFA6a-13Myc-KanMX6 plasmid (Longtine *et al.*, 1998) as template with the following primers: 1) CTCAAATAGGATAAAAAAAGGTTATATACAAATGCTTGGAAAAGAAATAAAAGTGGGGACGCTTATGAATTCGAGCTCGTTTAAAC and 2) CACACACAAGTGGATCAAAGTGAAGCACATATTGCAGGCCTAGAAAAGAAAAAGAAAAAGCAAAATAATCAACGGATCCCCGGGTTAATTAA was transformed into BJ4549 cells. Geneticin-resistant yeast colonies were selected and the integration site verified by PCR and sequence analysis. Western blot (WB) analysis indicates that a protein product of the expected size for Npr1-MYC is generated from this integration event.

The BJ5459 *npr1*Δ::*KanMX4* strain was constructed by PCR amplifying the *npr1*Δ::*KanMX4* deletion cassette from the BY4741 Open Biosystems (Rockford, IL) deletion collection (strain 2029) using the following primers: 1) GCCTACAAGGAGTTACGTGACATGCACG and 2) GCCTTGGTAAGACAATTAATGTTACCCGC.

The PCR product was transformed into BJ5459 cells and geneticin resistant colonies selected. Replacement of the chromosomal *NPR1* coding sequence with *KanMX* was verified by PCR.

Plasmids and DNA Manipulations

Plasmids used in this study and details of plasmid constructions are described in Supplemental Table 2. PCR amplifications were performed using HiFi Platinum Taq (Invitrogen, Beverly, MA), and all constructs were generated using PCR-based methods were confirmed by sequence analysis.

Citrulline Uptake Assays

Citrulline uptake assays were performed as described in Roberg *et al.* (1997b). Haploid cells from the *MAT***a** deletion collection were made prototrophic by transformation with pCK283 and one of the following: pRS426, pRS426-Aly1, or pRS426-Aly2. Cells were grown to ~3–4 × 10^6 c/ml in MIN-0.5% NH_4 medium, collected, and washed by filtration on a 0.45-μM HAWP filter (Millipore, Bedford, MA), and resuspended at 1×10^7 cells/ml in nitrogen-free medium before uptake assays. To initiate assays, 20 μM of ^{14}C-citrulline (Perkin Elmer-Cetus, Waltham, MA) was added to cells, and 100-μl aliquots were removed every 30 s over four time points. Cells were collected by filtration, washed, and placed in scintillation fluid to determine cellular incorporation of ^{14}C-citrulline. Assays were performed in triplicate, and the rate of citrulline uptake (DPM/min/OD_{600}) was determined. In each case, data are presented as the rate of citrulline uptake relative to the wild-type control. The average citrulline uptake of BY4741 prototrophic cells used in these assays was 3 nmol/min/OD_{600}, which is similar to that reported in Chen and Kaiser (2002). Error bars represent the SD of the mean.

β-Galactosidase Assays

Cells used in β-galactosidase assays with the YCp*GAP1-lacZ* reporter (Soussi-Boudekou and Andre, 1999) were grown to midlog phase in SC-0.5% NH_4 medium, washed and shifted into MIN-0.5% NH_4, MIN-0.1% GLN, or MIN-0.1% PRO for 3 h before cell harvest. Cell treatments were the same as those used before protein extractions for Gap1-green fluorescent protein (GFP) protein levels. β-Galactosidase assays were performed on three independent samples, and measurements were taken in triplicate as described in Bultynck *et al.* (2006). β-Galactosidase activity is reported as the maximum rate of OD_{415} change/min/amount of protein, and error bars represent the SD of the mean.

Fluorescence Microscopy

Cell imaging was performed with a Zeiss Axio Imager M1 microscope (Carl Zeiss, Jena, Germany), and images were captured with a Hamamatsu Orca-ER digital camera Bridgewater, NJ) coupled to Openlab Software 5.0.1 (Perkin Elmer-Cetus).

Homozygous diploid deletion strains (Open Biosystems) made prototrophic by transformation with pCKB230, pRS313, and one of pRS425, pRS425-

Aly1, or pRS425-Aly2 were used in Gap1-GFP imaging. Cells were grown in SC-0.5% NH_4 medium to ~1 × 10^7cells/ml, washed, resuspended in MIN-0.5% NH_4, and grown for 3 h at 23°C. Cells were immobilized on concanavalin A–treated coverslips, placed in a vacuum grease chamber, and visualized in growth medium. Exposure time, microscope settings, and image adjustments made using Adobe Photoshop (San Jose, CA) were consistent for all Gap1-GFP imaging from a given experiment, allowing for direct comparisons of Gap1-GFP intensities. In Adobe Photoshop an unsharp mask filter was applied (radius of 5 pixels) and the levels adjusted equivalently for all Gap1-GFP images. Quantification of Gap1-GFP intensity at the PM was performed using ImageJ 1.39u software (http://rsb.info.nih.gov/ij/; National Institutes of Health, Bethesda, MD). Cell PMs were traced, and the mean pixel intensity (fluorescence) for the PM was determined. A minimum of 150 cells was counted from five fields, and the intensities were normalized to the mean pixel intensity observed for the wild-type control cells. Error bars represent the SE of the mean.

To visualize GFP- or mCherry-tagged Aly1 or Aly2, cells were grown to ~1 × 10^7 cells/ml in SC-Met^- medium to induce arrestin expression, washed, and resuspended at ~1 × 10^8 cells/ml in GFP-kill buffer (Urbanowski and Piper, 1999) before visualization. Colocalization of GFP-tagged Aly1 and Aly2 with FM4-64 was performed as described in Foote and Nothwehr (2006). Quantification of colocalization was performed with ImageJ 1.39u software (National Institutes of Health) in a similar manner to that described in (Fernandez and Payne (2006). Images were converted to 8-bit and merged using the ImageJ Colocalizations plugin so that only foci in both channels were observed. A minimum of 90 cells and >200 Aly1- or Aly2-GFP foci were counted for each point. Percentage of foci colocalizing with FM4-64 out of the total number of Aly1 or Aly2 foci analyzed is presented.

Yeast Protein Purification and Immunoblotting

Copurification studies using glutathione *S*-transferase (GST)-fused Aly1 and Aly2 were performed by transforming BJ5459 or BJ5459-Npr1-MYC cells with pKK212, pKK212-Aly1, or pKK212-Aly2. Cells were grown to midlog phase in SC-Trp^- medium and induced to express GST, GST-Aly1, or GST-Aly2 from the *CUP1* promoter by adding 200 μM $CuSO_4$ and incubating for 1 h at 30°C. Protein extracts were obtained by glass-bead lysis in co-immunoprecipitation (CO-IP) buffer (50 mM Tris-HCl, pH 7.4, 15 mM EGTA, 100 mM NaCl, 0.2% Triton-X 100, with protease inhibitors), incubated for 2 h at 4°C with glutathione-Sepharose beads (GE Healthcare, Little Chalfont, Buckinghamshire, United Kingdom), washed three times in 500 μl of CO-IP buffer, aspirated to dryness, and eluted in Laemmli buffer.

Yeast protein extracts, not for use in copurification experiments, were obtained from sodium hydroxide cell lysis and tricholoroacetic acid precipitation of proteins using an equal number of cells as starting material (Volland *et al.*, 1994). Equal amounts of extracts were resolved by SDS-PAGE and transferred to nitrocellulose membrane for immunoblot analysis.

Immunoblots were probed with mouse monoclonal anti-GST (Covance, Emeryville, CA), mouse monoclonal anti-GFP (Covance), rabbit polyclonal anti-Myc (Covance), mouse monoclonal anti-Chc1 (gift from G. S. Payne, UCLA), rabbit polyclonal anti-Apl1 (gift from G. S. Payne), rabbit polyclonal anti-Apl2 (gift from G. S. Payne), and mouse monoclonal anti-Pgk1 (Molecular Probes, Carlsbad, CA) antibodies. In many experiments, Pgk1 is examined to ensure equivalent loading of extracts or input. To detect S-peptide–tagged proteins, the S-protein fused to horseradish peroxidase (HRP; Novagen, Madison, WI) was used. Anti-mouse and anti-rabbit secondary antibodies conjugated to HRP (GE Healthcare) and SuperSignal West Pico Chemiluminescent Substrate kit (Thermo Scientific, Rockford, IL) were used to detect immunoreactive bands, and multiple exposures of chemiluminescent signal to Kodak Biomax XAR film (Eastman Kodak, Rochester, NY) were taken for each blot.

Alternatively, for quantitative WB analysis anti-mouse and anti-rabbit secondary antibodies conjugated to Alexa flours (Invitrogen) were used, and images obtained using an Odyssey imager and software (LI-COR Biosciences, Lincoln, NE). Quantification of WBs was performed using ImageJ 1.39u software (National Institutes of Health).

GST-Npr1 used for in vitro kinase assays was purified from Y258 yeast cells (Zhu *et al.*, 2001) by glass-bead lysis in (50 mM Tris-HCl, pH 7.5, 100 mM NaCl, 1 mM EGTA, 0.1% Triton X-100, 0.1% β-mercaptoethanol) with protease inhibitors and binding to glutathione-Sepharose beads (GE Healthcare). Glutathione-bound GST-Npr1 was washed three times in the same buffer as used in the lysis with the addition of 750 mM NaCl and 1% Triton X-100 (to help limit the number of proteins copurifying with Npr1), eluted off beads in this buffer with 10 mM reduced glutathione and dialyzed in phosphate-buffered saline (PBS; 80.2 mM K_2HPO_4, 19.8 mM KH_2PO_4, 150 mM NaCl) overnight. To ensure resolution of Npr1 (which autophosphorylates) from pET-Aly2, the GST tag was removed via thrombin digestion (incubated with 3 pg/μl thrombin at 4°C overnight). Cleaved GST and uncleaved GST-Npr1 were removed by incubation with glutathione-Sepharose beads, and the unbound, cleaved Npr1 was dialyzed overnight in PBS.

Bacterial Protein Purifications

pGEX-KG, pGPB1013, pGPB828, and pGPB1025 (Yeung and Payne, 2001) were transformed into BL21-DE3 pLys (Invitrogen) *Escherichia coli*. Cultures were grown to OD_{600} = 1.0 at 37°C, induced to express GST-fusion proteins with 1 mM isopropyl β-D-1-thiogalactopyranoside (IPTG), and grown an additional 2 h at 37°C. Cell lysates were generated by sonication in PBS with protease inhibitors. After lysis, 1% Triton X-100 was added, and insoluble material removed by two sequential centrifugations at 15,000 × *g* for 20 min. GST-proteins were purified on glutathione-Sepharose beads and washed in PBS with an additional 500 mM NaCl.

pET-fusion constructs for Aly1 and Aly2 were transformed into BL21-DE3 Star (Invitrogen) *E. coli*. Cultures were grown to OD_{600} = 1.0 at 30°C, induced to express pET-fusion proteins with 1 mM IPTG, and grown an additional 5 h at 23°C. Cell lysates were generated by sonication in extraction buffer (50 mM Tris-HCl, pH 8, 300 mM NaCl, 0.1% NP-40, 10 mM imidazole, PMSF and benzamidine) followed by two sequential centrifugations at 15,000 × *g* for 20 min to remove insoluble material. pET-fusion proteins were purified on Ni-NTA agarose (5 PRIME, Hamburg, Germany), washed with 20 bed-volumes of wash buffer (same as extraction buffer with 20 mM imidazole), and eluted in two-bed volumes of elution buffer (same as extraction buffer with 250 mM imidazole). Proteins were dialyzed overnight in PBS before use in copurification studies.

In Vitro Kinase Assays

pET and pET-Aly2 were incubated for 30 min at 30°C in kinase buffer (50 mM Tris-HCl, pH 7.5, 20 mM $MgCl_2$, 1 mM DTT, 1 μM unlabeled ATP, aprotinin, and leupeptin) with 75 nM [γ-^{32}P]ATP (Perkin Elmer-Cetus) with or without Npr1 kinase (purified from Y258 yeast cells). Unincorporated ^{32}P was removed using a Centri-Sep spin column (Princeton Separations, Adelphia, NJ). Protein samples were resolved on 4–15% acrylamide gels by SDS-PAGE. Gels were stained with Gel Code Blue (Bio-Rad, Hercules, CA) or dried, exposed to a phosphoimager screen, and imaged with a Typhoon scanner (GE Healthcare).

RESULTS

Aly1 and Aly2 Regulate Yeast Response to Nitrogen Starvation

We sought to identify trafficking functions for the uncharacterized α-arrestins, Aly1 and Aly2. Other α-arrestins regulate nutrient permeases; to determine if Aly1 and Aly2 regulate nutrient responses, we examined the growth of *aly1*Δ or *aly2*Δ cells in the presence of rapamycin, a TORC1-inhibitor that mimics nitrogen starvation (Zheng *et al.*, 1995). *aly1*Δ and *aly2*Δ cells were sensitive to this drug, whereas cells overexpressing *ALY1* or *ALY2* were rapamycin resistant (Figure 1A). *aly1*Δ *aly2*Δ cells were more sensitive to rapamycin than either single mutant. Thus, these gene products promote growth under nitrogen limiting conditions and may function in distinct pathways.

When nitrogen is limiting, yeast import and metabolize amino acids as a nitrogen source. To test if Aly1 and Aly2 alter amino acid uptake, we monitored growth of *aly1*Δ or *aly2*Δ mutants in the presence of toxic amino acid analogs. Cells lacking *ALY1* and/or *ALY2* were resistant to AzC and canavanine, toxic analogs of proline and arginine, respectively (Figure 1B). Conversely, cells overexpressing *ALY1* or *ALY2* were sensitive to these compounds (Figure 1B). These phenotypes suggest that Aly1 and Aly2 elevate cell surface localization and/or activity of the permeases required for analog uptake. AzC enters cells through several permeases, including Gap1 and Put4, whereas canavanine enters via the Can1 permease (Grenson *et al.*, 1966; Andreasson *et al.*, 2004). Nitrogen-dependent regulation of Gap1 trafficking is well characterized; therefore, we next examined whether Aly1 and Aly2 influence activity of this permease. Gap1 activity at the cell surface was determined in cells lacking or overexpressing *ALY1* and/or *ALY2* by measuring uptake of [^{14}C]citrulline, which is transported exclusively by Gap1 (Grenson *et al.*, 1970; Figure S1A). [^{14}C]citrulline uptake in *aly1*Δ, *aly2*Δ, or *aly1*Δ *aly2*Δ cells occurs at half the rate of wild-type cells (Figure 1C and Figure S1A), whereas cells overexpressing *ALY1* or *ALY2* transported citrulline at almost twice the rate of vector control cells (Figure 1D). Thus, Aly1 and Aly2 increase Gap1 activity and/or levels

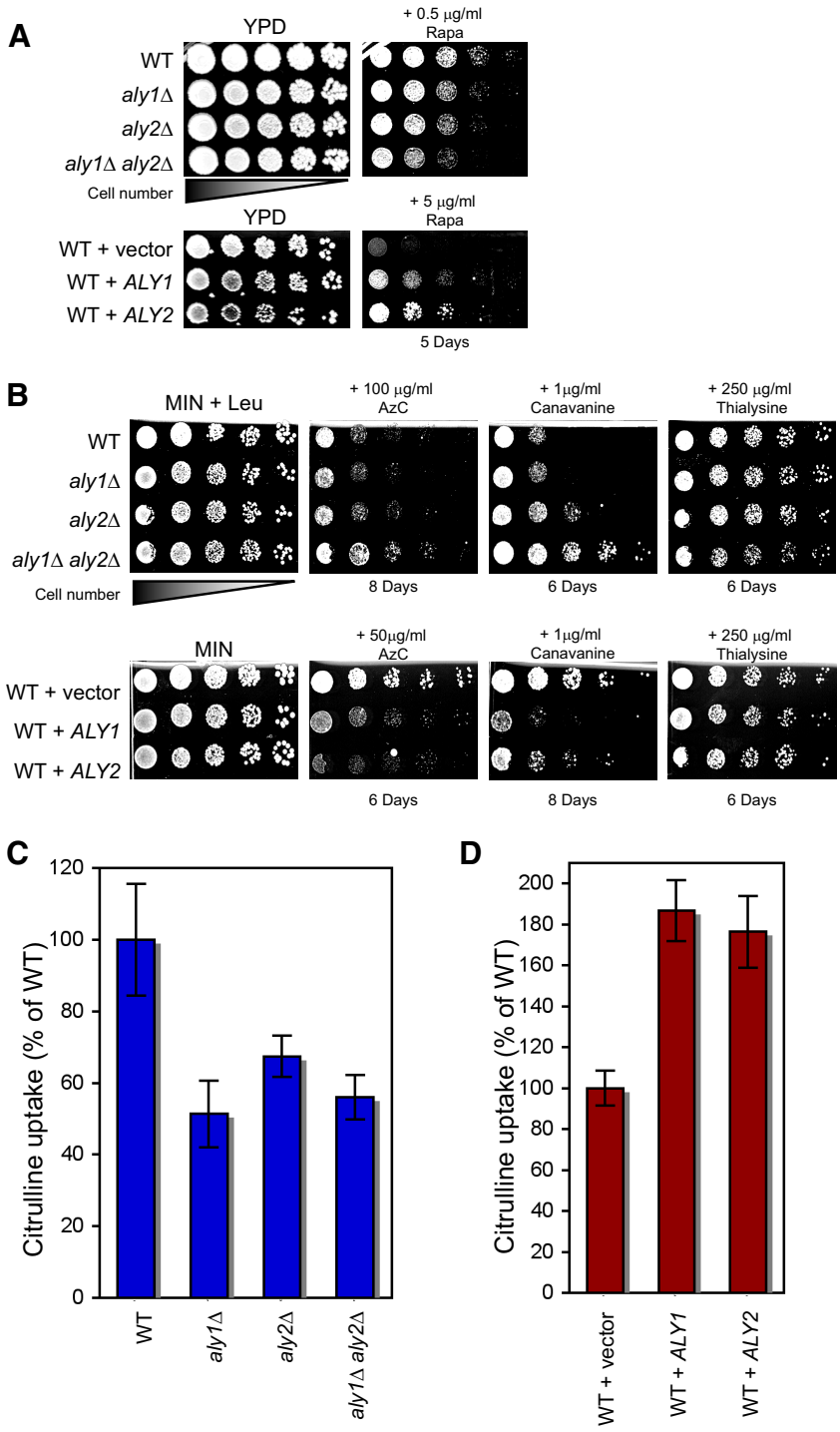

Figure 1. Aly1 and Aly2 assist in adaptation to nitrogen starvation. (A) Growth of wild-type (WT; BY4741), *aly1*Δ (5092), *aly2*Δ (1339), and *aly1*Δ *aly2*Δ (D2–6A) or WT cells with pRS426, -*ALY1* or -*ALY2* on YEPD ± rapamycin. (B) Growth of WT (BY4741), *aly1*Δ (5092), *aly2*Δ (1339), and *aly1*Δ *aly2*Δ (D2–6A) or WT cells with pRS425, -*ALY1* or -*ALY2* on MIN-0.25% NH_4 ± amino acid analog. (C) WT (BY4741), *aly1*Δ (5092), *aly2*Δ (1339), and *aly1*Δ *aly2*Δ (D2–6A) with pCK283 and pRS426 or (D) WT (BY4741) cells with pCK283 and pRS426, -*ALY1*, or -*ALY2* were assayed for [^{14}C]citrulline uptake. The mean uptake rate ± SDM for three replicates is shown as % relative to WT.

at the PM and may regulate additional permeases (e.g., Can1 and Put4). However, Aly1 and Aly2 affect only a subset of permeases, as cells lacking or overexpressing *ALY1* and/or *ALY2* grew equivalently to wild-type cells in the presence of thialysine, a toxic lysine analog imported by Lyp1 (Grenson *et al.*, 1966; Figure 1B). Increased Gap1 transport activity upon Aly1 or Aly2 overexpression is inconsistent with a role for Aly1 and Aly2 in promoting Gap1 endocytosis and rather suggests a novel function for these arrestins in increasing the amount of PM-localized Gap1.

Aly1 and Aly2 Copurify with Gap1 and Increase Gap1 Levels

To test if Aly1 and Aly2 interact with Gap1, GST-fused Aly1 or Aly2 was isolated from extracts of cells expressing Gap1-GFP. Aly1 and Aly2 both copurified with Gap1 (Figure 2A), suggesting that they act directly on this permease to alter its activity and/or levels at the PM.

Gap1 trafficking is well characterized making it an excellent model for exploring Aly1 and Aly2 trafficking functions. Gap1 is a high-affinity transporter for a broad spectrum of amino

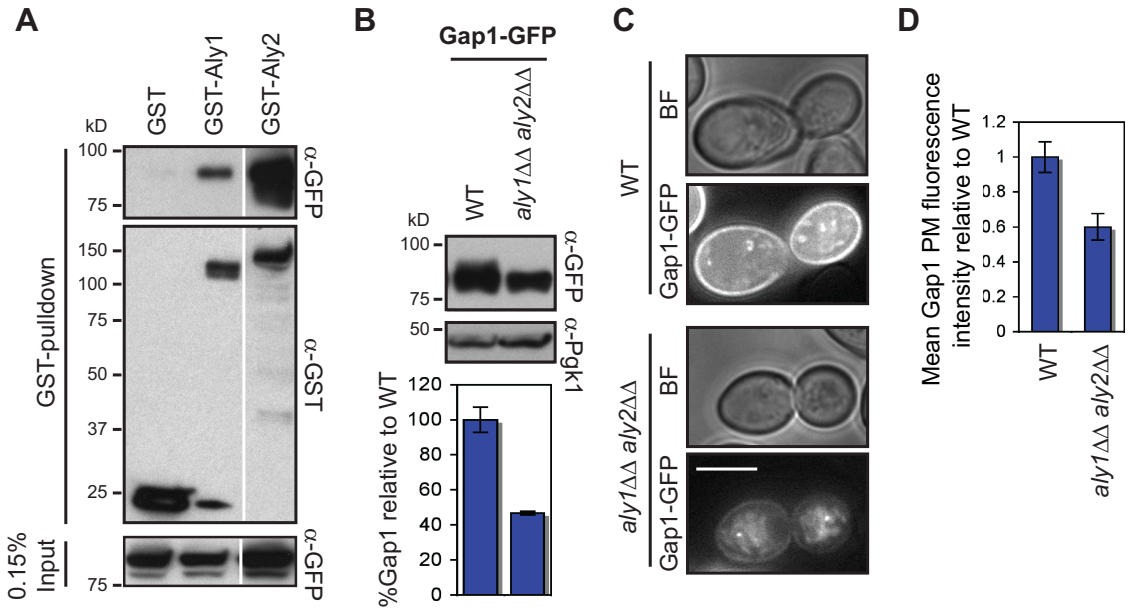

Figure 2. Aly1 and Aly2 interact with and increase Gap1 levels. (A) GST (pKK212), GST-Aly1 (pKK212-Aly1), and GST-Aly2 (pKK212-Aly2) were purified from Gap1-GFP (pAR13) containing BJ5459 cells grown in SC-0.1% PRO and copurification assessed by WB. Samples were run on one gel, but line denotes lane removal. (B) Extracts from prototrophic WT (BY4743) or *aly1*ΔΔ *aly2*ΔΔ cells with Gap1-GFP (pCK230), pRS313 and pRS425 grown in SC-0.5% NH_4, washed, and grown for 3 h in MIN-0.5% NH_4 were assessed by WB. The mean band intensity for three replicates ± SDM is plotted relative to the WT. (C and D) The same cells as in B were visualized using fluorescence microscopy (scale bar, 5 μm; C), and PM fluorescence intensity was quantified (D). Mean PM fluorescence intensity ± SEM is plotted relative to WT.

acids, which can be scavenged for use as a nitrogen source. Cells grown on a preferred nitrogen source, such as glutamine, do not require PM-localized Gap1, and newly synthesized Gap1 is sorted from the *trans*-Golgi network (TGN) to endosomes and on to the vacuole for degradation (Figure 3A). This TGN-to-vacuole sorting of Gap1 is regulated by Bul1 and Bul2, two adaptors for the Rsp5-ubiqutin ligase, and requires polyubiquitination of Gap1 by Rsp5 (Helliwell *et al.*, 2001; Soetens *et al.*, 2001; Lauwers *et al.*, 2009). In cells grown on a poor nitrogen source, such as proline, Gap1 traffics from the TGN to the PM, where it assists in nitrogen uptake (Figure 3A). Nitrogen supply also regulates Gap1 recycling from endosomes to the TGN; preferred nitrogen sources inhibit recycling, whereas amino acid starvation or growth on a poor nitrogen source activates recycling (Rubio-Texeira and Kaiser, 2006; Figure 3A). Finally, nutrients regulate Gap1 endocytosis with addition of high concentrations of amino acids or a preferred nitrogen source triggering permease internalization (De Craene *et al.*, 2001; Risinger and Kaiser, 2008). We monitored the impact of Aly1 and Aly2 on Gap1 trafficking under a range of nutrient conditions.

We examined Gap1-GFP levels and localization in *aly1*Δ *aly2*Δ cells under conditions that allow Gap1 localization to the PM (i.e., growth in amino acid–free medium with ammonium (NH_4), an intermediate quality nitrogen source that allows some Gap1 delivery to the PM and some to the MVB-vacuole; see Figure 3A). Compared with wild-type cells, levels of total (Figure 2B) and PM-localized Gap1-GFP (Figure 2, C and D) were reduced by twofold in *aly1*Δ *aly2*Δ cells. Thus, in *aly1*Δ *aly2*Δ cells the slower citrulline uptake rates (Figure 1C) can be explained by reduced amounts of Gap1 at the PM.

Gap1 protein levels are not only altered by changes in its trafficking, but are also altered by nutrient-regulated changes in *GAP1* gene expression. To determine whether Aly1 or Aly2 modulate *GAP1* transcription, we monitored expression of a *GAP1* promoter-*lacZ* fusion (Soussi-Boudekou and Andre, 1999). Neither deletion nor overexpression of *ALY1* or *ALY2* affected activity of the P_{GAP1}-*lacZ* reporter under any condition used in these studies (Figures S1, B–D). Thus, Aly1 and Aly2 interact with Gap1 and act posttranscriptionally to increase Gap1 protein levels, including Gap1 at the PM.

Aly1 and Aly2 Do Not Influence Gap1 Endocytosis

Decreased total and PM-localized Gap1 in *aly1*Δ *aly2*Δ cells indicates that more Gap1 traffics to the vacuole in this strain. Increased vacuolar degradation of Gap1 could result from: 1) increased endocytosis, 2) impaired Gap1 trafficking from the trans-Golgi network (TGN) to the PM, or 3) impaired Gap1 recycling from endosomes to the TGN. To determine which of these is operative, we first examined endocytosis of Gap1 in wild-type and *aly1*Δ *aly2*Δ cells under conditions that allow Gap1 trafficking to the PM (Figure 3B). Gap1-GFP levels were monitored in cycloheximide-treated cells after addition of casamino acids, which triggers endocytosis and inhibits endosome-TGN recycling (Risinger and Kaiser, 2008) (Figure 3A). Under these conditions, Gap1 degradation occurs predominantly through endocytic turnover, and this is unchanged in *aly1*Δ *aly2*Δ cells (Figure 3B). Thus, Gap1 reduction in *aly1*Δ *aly2*Δ cells is not due to increased endocytosis. Consistent with this conclusion, *ALY1* and *ALY2* overexpression increased AzC sensitivity equivalently in wild-type and *end3*Δ cells, which are defective for Gap1 endocytosis (Nikko *et al.*, 2003) (Figure S2A). Therefore, Aly1 and Aly2 increase Gap1 levels through an endocytosis-independent mechanism.

Aly1 and Aly2 Are Not Required for Gap1 Delivery from the TGN to the PM

Next, we investigated effects of Aly1 and Aly2 on Gap1 trafficking under two different nutrient conditions. First, Gap1 levels were examined in cells grown on proline, a poor nitrogen source that stimulates Gap1 trafficking from the TGN-to-PM and inhibits its delivery to the MVB/vacuole (Figure 3A). Growth in proline results in much higher Gap1

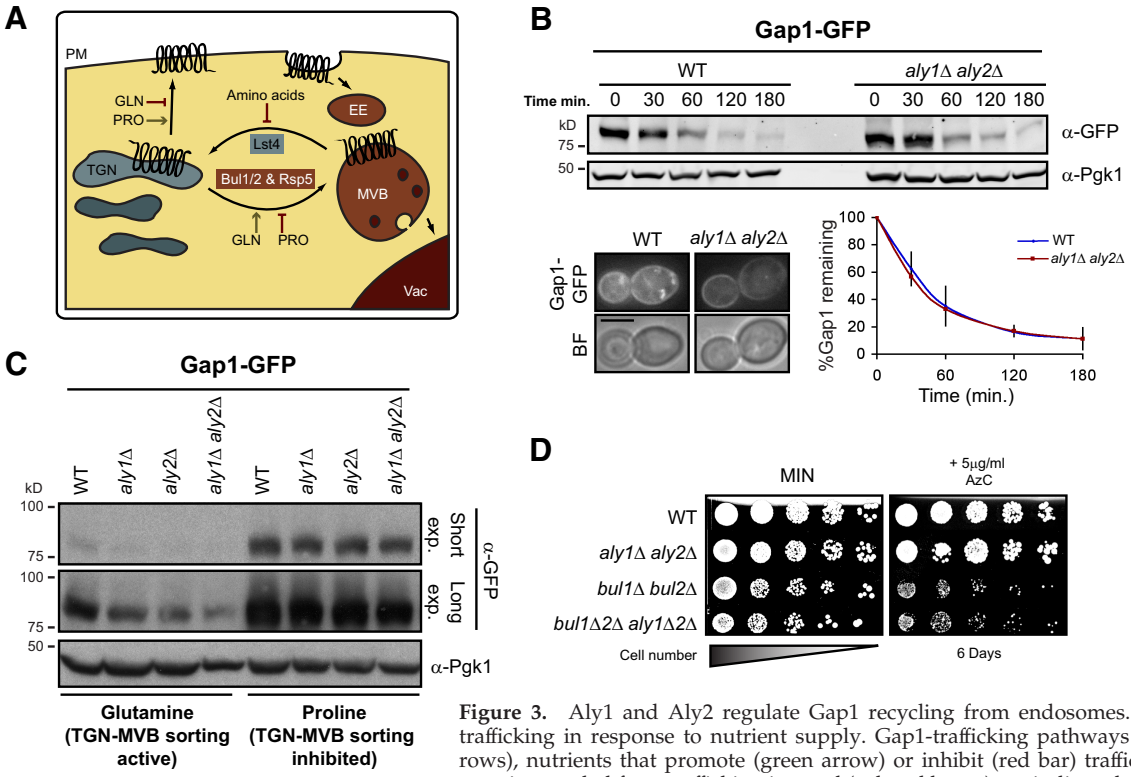

Figure 3. Aly1 and Aly2 regulate Gap1 recycling from endosomes. (A) Gap1 trafficking in response to nutrient supply. Gap1-trafficking pathways (black arrows), nutrients that promote (green arrow) or inhibit (red bar) trafficking, and proteins needed for a trafficking interval (colored boxes) are indicated. Growth in glutamine (GLN), a preferred nitrogen source, inhibits Gap1 delivery to PM and promotes TGN-to-MVB/vacuole trafficking by stimulating polyubiquitination of Gap1 by Bul1/Bul2/Rsp5 (Helliwell *et al.*, 2001; Soetens *et al.*, 2001; Lauwers *et al.*, 2009). Growth in proline (PRO), a poor nitrogen source, promotes Gap1 TGN-to-PM trafficking and inhibits TGN-to-MVB/vacuole trafficking. Gap1 recycling from endosomes-to-TGN requires Lst4 and is inhibited by amino acids (Roberg *et al.*, 1997a; Rubio-Texeira and Kaiser, 2006). Gap1 at the PM undergoes Rsp5-dependent endocytosis when amino acids or a preferred nitrogen source are added (De Craene *et al.*, 2001; Risinger and Kaiser, 2008). For most of our experiments, cells were grown in NH_4, a nitrogen source of intermediate quality. Under these conditions, some Gap1 is delivered to the PM and some is delivered to the MVB/vacuole for degradation. EE, early endosome; Vac, vacuole. (B) WT (BY4741) or *aly1Δaly2Δ* (D2–6A) cells with Gap1-GFP (pCK230) were grown in MIN-0.2% urea and incubated with 50 μg/ml CHX for 20 min. At 0 min (Gap1 localization shown; scale bar, 5 μm), 0.1% casamino acids was added to trigger Gap1 endocytosis. Band intensities were measured, and the mean % of Gap1 remaining, as determined from three replicates, is shown ±SDM. Growth in MIN-0.5% NH_4 gave similar results (data not shown). (C) Extracts from WT (BY4741), *aly1Δ* (5092), *aly2Δ* (1339), and *aly1Δaly2Δ* (D2–6A) cells with Gap1-GFP (pCK230) grown in SC-0.5% NH_4, washed, and grown for 3 h in MIN-0.1% GLN or MIN-0.1% PRO were assessed by WB. The two exposures shown, 1 min short exp. and 10 min long exp., allow comparison of protein levels. (D) Growth of WT (BY4741), *aly1Δ::NatMX4 aly2Δ::URA3*, *bul1Δ bul2Δ* (spore 3A), and *bul1Δ bul2Δ aly1Δ aly2Δ* (spore 7D) on MIN-0.5% NH_4 ± AzC. (E) WT (BY4741) or *aly1Δ aly2Δ* (D2–6A) cells with pCK283 and pRS426 were grown in either MIN-0.1% GLN or MIN-0.1% glutamate (GLU), transferred to MIN-0.1% urea with 1.5 μg/ml CHX and the kinetics of Gap1 trafficking to the PM monitored by [^{14}C]citrulline uptake. The mean uptake rate (DPM/min/OD_{600}) for two independent samples ± SEM is plotted.

levels than growth in glutamine, a preferred nitrogen source that promotes TGN sorting of Gap1 to the MVB (Figure 3A). Loss of *ALY1* and *ALY2* had little effect on Gap1 levels in proline-grown cells (Figure 3C; short exp.), which is inconsistent with roles for these proteins in delivering Gap1 from the TGN to the PM. In contrast, Gap1 was significantly reduced in *aly1Δ aly2Δ* cells grown in glutamine, suggesting that Aly1 and Aly2 influence Gap1 abundance only when TGN-to-MVB sorting of the permease is active (Figure 3C; long exp., and see next section).

We also examined Aly1 and Aly2 function in cells lacking Bul1 and Bul2, Rsp5-adaptors that promote polyubiquitination of Gap1 and that are required for delivery of the permease to the vacuole (Helliwell *et al.*, 2001; Soetens *et al.*, 2001; Lauwers *et al.*, 2009; Figure 3A). In *bul1Δ bul2Δ* cells, Gap1 is constitutively delivered to the PM, resulting in severe AzC sensitivity (Helliwell *et al.*, 2001; Soetens *et al.*, 2001; Figure 3D). We found that *bul1Δ bul2Δ* and *aly1Δ aly2Δ bul1Δ bul2Δ* cells displayed equivalent sensitivity to AzC (Figure 3D). Thus, under two different conditions where TGN-to-PM trafficking of Gap1 predominates, loss of Aly1 and Aly2 have little effect on Gap1 levels or activity. We conclude that Aly1 and Aly2 are not required for TGN-to-PM trafficking of Gap1.

Aly1 and Aly2 Promote Amino Acid–regulated Recycling of Gap1 from Endosomes

The findings described above are consistent with functions for Aly1 and Aly2 in endosomal recycling of Gap1. First, loss of

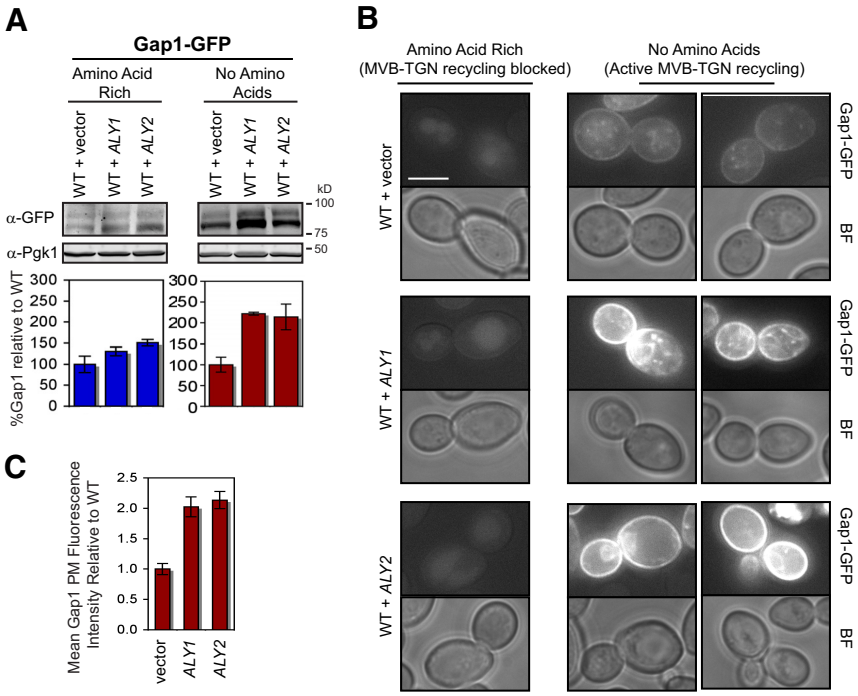

Figure 4. Aly1 and Aly2 regulate Gap1 recycling in response to amino acid starvation. (A) Extracts from prototrophic WT (BY4743) cells with Gap1-GFP (pCK230), pRS313 and pRS425, -Aly1 or -Aly2 grown in SC-0.5% NH_4 (Amino Acid Rich/MVB-TGN recycling inhibited), washed, and grown for 3 h in MIN-0.5% NH_4 (No Amino Acids/MVB-TGN recycling active) were assessed by WB. The mean band intensity for three replicates ± SDM is plotted relative to the WT. (B and C) Cells grown as in A were B visualized using fluorescence microscopy (scale bar, 5 μm), and (C) the mean Gap1 PM fluorescence intensity (for MIN-0.5% NH_4 grown cells) ± SEM is plotted relative to WT.

Aly1 and Aly2 significantly decreased Gap1 levels in glutamine-grown cells (Figure 3C, long exp.), where Gap1 cycling from endosomes to the TGN contributes significantly to steady-state levels by rescuing Gap1 from vacuolar degradation (Rubio-Texeira and Kaiser, 2006; Risinger and Kaiser, 2008). In proline-grown cells, where recycling from endosomes is inhibited, loss of Aly1 and Aly2 had little effect on Gap1 levels. Second, previous work has shown that mutations compromising the MVB-to-TGN recycling of Gap1 have no effect in *bul1*Δ *bul2*Δ cells, because deleting *BUL1* and *BUL2* blocks Gap1 delivery to the MVB and eliminates the pool of Gap1 acted on by recycling proteins (Helliwell *et al.*, 2001; Risinger *et al.*, 2006; Rubio-Texeira and Kaiser, 2006). As described above, *aly1*Δ *aly2*Δ, similar to other recycling mutants, do not alter AzC sensitivity of *bul1*Δ *bul2*Δ (Figure 3D).

Observations in *vps4*Δ cells also suggested that Aly1 and Aly2 function in endosomal recycling (Figure S2, B and C). In *vps4*Δ cells the ESCRT-III complex and MVB formation are defective, resulting in inefficient degradation of Gap1. Gap1 accumulates in aberrant, prevacuolar "class E" compartments (Raymond *et al.*, 1992) from which it recycles to the PM causing AzC sensitivity (Rubio-Texeira and Kaiser, 2006). *aly1*Δ *aly2*Δ *vps4*Δ cells are less sensitive to AzC than *vps4*Δ cells, indicating that Gap1 recycling is partially dependent on Aly1 and Aly2 (Figure S2B), whereas overexpression of *ALY1* and *ALY2* in *vps4*Δ cells increases AzC sensitivity (Figure S2C), consistent with a role for Aly proteins in recycling Gap1 from the class E, prevacuolar compartment.

To examine nutrient-regulated endosomal recycling of Gap1 directly, Gap1 activity was monitored after transferring cells grown in glutamate (a good nitrogen source) to medium containing urea (a poor nitrogen source) and cycloheximide (CHX). These conditions trigger redistribution of Gap1 from intracellular reserves to the PM while preventing new Gap1 synthesis (Roberg *et al.*, 1997b). In wild-type cells transferred from glutamate to urea/CHX, [^{14}C]citrulline uptake increased quickly and peaked at 15 min, indicating efficient redistribution of Gap1 from intracellular stores to the PM (Figure 3E). In contrast, no increase in Gap1 activity at the PM was observed for *aly1*Δ *aly2*Δ cells under these conditions, indicating that Aly1 and Aly2 are important for maintaining intracellular Gap1 and/or delivering Gap1 from intracellular stores to the PM (either directly or through intermediate compartments such as the TGN), in response to nutrients. No uptake was observed for either wild-type or *aly1*Δ *aly2*Δ cells shifted from glutamine to urea/CHX, because synthesis of Gap1 protein is required to restore activity under these conditions (Roberg *et al.*, 1997b; Figure 3E).

Amino acids inhibit recycling of Gap1 from endosomes (Rubio-Texeira and Kaiser, 2006). Therefore, we examined Gap1 in cells overexpressing *ALY1* or *ALY2* that were grown in amino acid–rich medium and transferred to amino acid–free medium, which releases the recycling block (Figure 3A). *ALY1* or *ALY2* overexpression had no significant effect on Gap1 levels or localization when recycling was inhibited (Figure 4, A and B). However, when endosome-to-TGN recycling was active, *ALY1* and *ALY2* overexpression caused a twofold increase in Gap1 abundance (Figure 4A), resulting in higher Gap1 levels at the PM and in intracellular compartments as determined by fluorescence microscopy (Figure 4, B and C). This twofold increase in Gap1 levels at the PM when *ALY1* or *ALY2* are overexpressed (Figure 4C) is supported by the twofold increase in citrulline uptake observed under these same conditions (Figure 1D). Consistent with the *ALY1* and *ALY2* overexpression results (Figure 4, A–C), when endosome-to-TGN recycling is active *aly1*Δ *aly2*Δ cells displayed reduced levels of total and PM-localized Gap1-GFP compared with wild-type cells (Figure 2, B–D).

These data support a role for Aly1 and Aly2 in the nutrient-regulated recycling of Gap1 from endosomes to the TGN and/or PM. By promoting Gap1 recycling, Aly1 and Aly2 rescue Gap1 from vacuolar-degradation pathways and increase Gap1 protein levels, both within internal membranes and at the PM. These findings establish a novel function for arrestins as regulators of intracellular protein sorting.

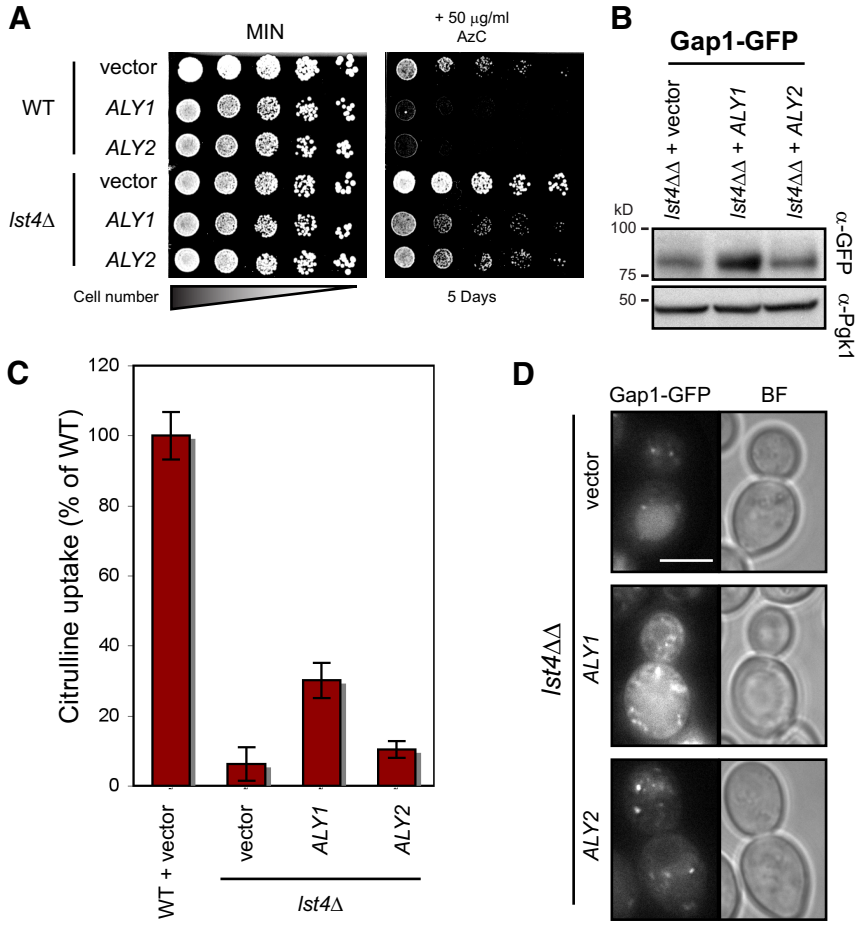

Figure 5. Aly1, but not Aly2, restores Gap1 PM-localization in *lst4*Δ. (A) Growth of WT (BY4741) or *lst4*Δ (5026) cells with pRS425, pRS425-Aly1, or pRS425-Aly2 on MIN-0.5% NH_4 ± AzC. (B and D) Prototrophic *lst4*ΔΔ (35026) cells with pCK230 (Gap1-GFP), pRS313, and pRS425, -Aly1, or -Aly2 were grown in SC-0.5% NH_4, washed, and grown for 3 h in MIN-0.5% NH_4. (B) Cell extracts were assessed by WB. (D) Gap1-GFP was visualized by fluorescence microscopy (scale bar, 5 μm). (C) Prototrophic WT (BY4741) and *lst4*Δ (5026) cells with pCK283 and pRS426, -*ALY1*, or -*ALY2* were assayed for [^{14}C]citrulline uptake. The mean uptake rate ± SDM for three replicates is shown as % relative to WT.

Aly2-mediated Gap1 Recycling Requires Lst4

We next sought to determine if Aly1 or Aly2 regulate Gap1 in conjunction with other Gap1 recycling factors. Lst4 promotes an amino acid–regulated Gap1 recycling pathway from endosomes to the PM, proposed to transit through a TGN intermediate (Roberg *et al.*, 1997a; Rubio-Texeira and Kaiser, 2006; Figures 3A and 9). In *lst4*Δ cells, Gap1 is constitutively sorted to the vacuole and degraded resulting in resistance to AzC (Figure 5A) and a 10-fold reduction Gap1 activity compared with wild-type cells (Roberg *et al.*, 1997a; Rubio-Texeira and Kaiser, 2006; Figure 5C and Figure S1A). To determine if Aly1 and Aly2 influence Gap1 trafficking through an Lst4-dependent or independent mechanism, we explored the effects of overexpressing *Aly1* or *Aly2* in *lst4*Δ cells.

Overexpression of *ALY1* in *lst4*Δ mutants increased sensitivity to AzC compared with vector-containing cells (Figure 5A). In addition, *ALY1* overexpression increased Gap1 levels (Figure 5B), Gap1 activity (fivefold faster rate of citrulline uptake compared with the *lst4*Δ with vector control; Figure 5C), and PM-localization of Gap1 (Figure 5D) in *lst4*Δ cells. These data indicate that Aly1 regulates an Lst4-independent Gap1 trafficking pathway that partially bypasses vacuolar sorting of Gap1 in *lst4*Δ cells. In marked contrast, *ALY2* overexpression in *lst4*Δ cells failed to confer the same degree of AzC sensitivity as *ALY1* overexpression (Figure 5A) and failed to increase Gap1 levels (Figure 5B), activity (Figure 5C), or PM localization (Figure 5D) in comparison with *lst4*Δ containing a vector control. Thus, in contrast to Aly1, Aly2 primarily influences Lst4-dependent Gap1-trafficking (see Figure 9).

Aly2 Interacts with and Requires Npr1 to Mediate Gap1 Trafficking

Npr1, the nutrient permease reactivator kinase, is active under nitrogen-limiting conditions and is inhibited in a TORC1-dependent manner during growth in preferred nitrogen (Schmidt *et al.*, 1998). Npr1 is required for Gap1 targeting to the PM, although substrates that mediate this regulation have not been identified (De Craene *et al.*, 2001). Analysis of Aly1 and Aly2 copurifying proteins by mass spectrometry (MS) identified Npr1 peptides in Aly2-, but not Aly1-containing complexes (data not shown). We verified the Aly2-Npr1 interaction by reciprocal copurifications with chromosomally Myc-tagged Npr1 and GST-fused Aly2, under both good and poor nitrogen conditions (Figure 6A and data not shown). In contrast, Npr1-Myc did not copurify with GST or GST-Aly1 under any of the nutrient conditions tested (Figure 6A and data not shown).

To explore possible functional interactions between Npr1, Aly1, and Aly2, we examined the impact of *ALY1* and *ALY2* overexpression on *npr1*Δ cells. *npr1*Δ cells constitutively deliver Gap1 to the vacuole under all nutrient conditions and so have less Gap1 at the PM, cannot utilize citrulline as a nitrogen source, and are resistant to AzC (De Craene *et al.*, 2001; Soetens *et al.*, 2001; Boeckstaens *et al.*, 2007). Overexpression of *ALY1* in *npr1*Δ cells rescued growth on citrulline as a nitrogen source (Figure 6B) and increased AzC sensitivity (Figure 6C), Gap1 activity (2.5-fold) (Figure 6D), Gap1 levels (Figure 6E), and Gap1 localization to intracellular patches and the PM (Figure 6F) in comparison to vector-containing cells. In contrast, *Aly2* overexpression failed to

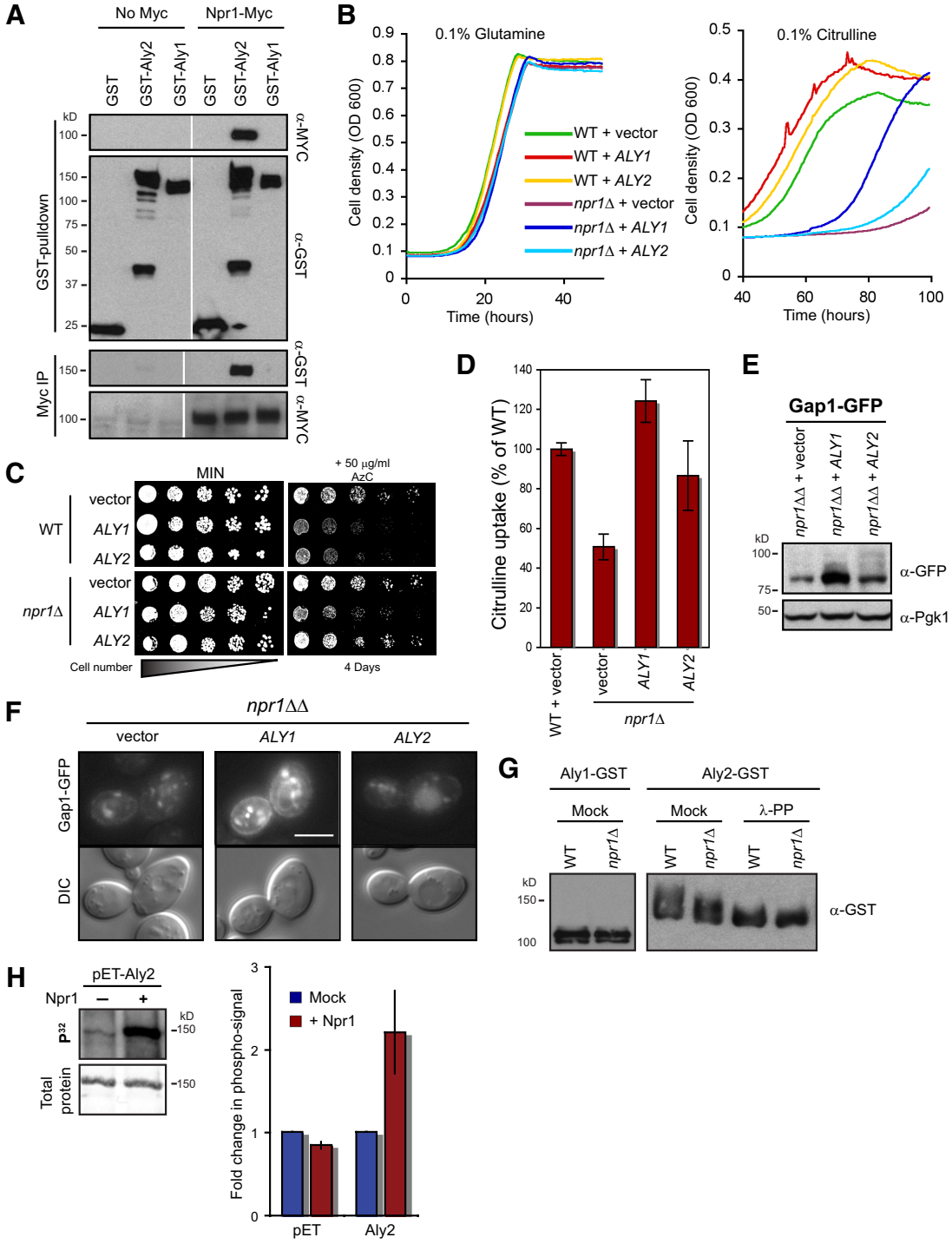

Figure 6. Aly2 interacts with and requires Npr1 to promote Gap1 PM-localization. (A) BJ5459 or BJ5459-Npr1-MYC cells expressing GST (pKK212), GST-Aly1 (pKK212-Aly1), or GST-Aly2 (pKK212-Aly2) were grown in SC-0.25% NH_4. Protein extracts were split, with half used for GST and half for anti-MYC Ab purifications, and copurification assessed by WB. Samples were run on one gel, but line denotes lane removal. (B) WT (BY4741) or *npr1*Δ (2029) cells with pRS425, -Aly1 or -Aly2 were grown in MIN-0.25% NH_4, washed, and inoculated at equal density into either MIN-0.1% GLN or MIN-0.1% citrulline (CIT). Growth was monitored using OD_{600} readings, taken every 30 min with a Tecan Genios microtiter plate reader. (C) Growth of WT (BY4741) or *npr1*Δ (2029) cells with pRS425, -Aly1, or -Aly2 on MIN-0.5% NH_4 ± AzC. (D) Prototrophic WT (BY4741) and *npr1*Δ (2029) with pCK283 and pRS426, *-ALY1*, or *-ALY2* were assayed for [^{14}C]citrulline uptake. The mean uptake rate ± SDM for three replicates is shown as % relative to WT. (E and F) Prototrophic *npr1*ΔΔ (32029) cells with Gap1-GFP (pCK230), pRS313 and pRS425, -Aly1, or -Aly2 were grown in SC-0.5% NH_4, washed, and grown for 3 h in MIN-0.5% NH_4 and (E) cell extracts were assessed by WB or (F) Gap1-GFP was visualized using fluorescence microscopy (scale bar, 5 μm). (G) GST-Aly1 (pKK212-Aly1) or -Aly2 (pKK212-Aly2) were purified from extracts of WT (BJ5459) or *npr1*Δ (BJ5459-*npr1*Δ::*KanMX*) cells grown in SC-0.25% NH_4 and assessed by WB. Similar results were obtained using GFP-Aly1 and -Aly2 extracted from WT (BY4741) or *npr1*Δ (2029) cells (data not shown). Phosphorylation of GST-Aly2 was further analyzed using mock (−) or lambda phosphatase treatment (λ-PP). (H) pET and pET-Aly2 were purified from *E. coli* and incubated with [γ-^{32}P]ATP kinase cocktail in the presence (+) or absence (−) of Npr1. Proteins were analyzed by

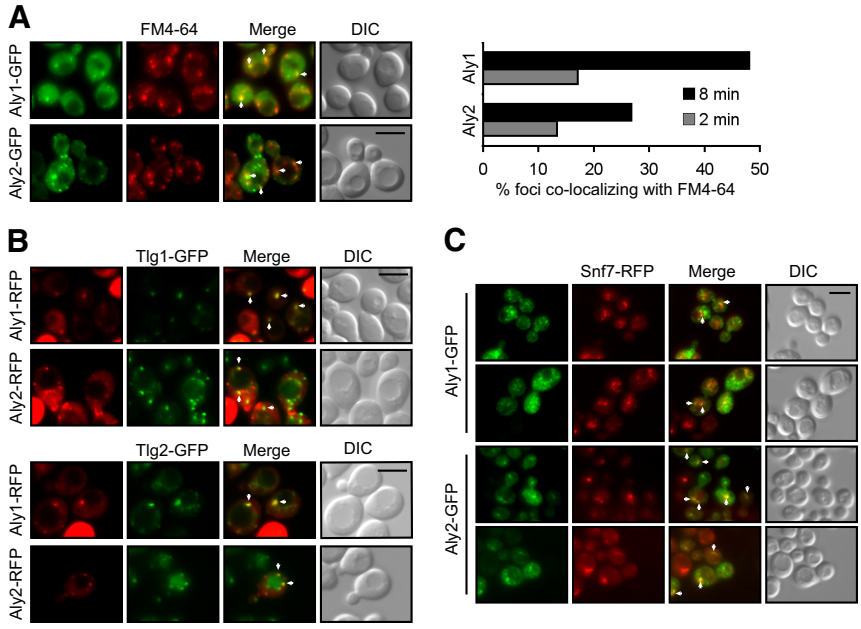

Figure 7. Aly1 and Aly2 localize to endosomes. (A) Colocalization of FM4-64–stained compartments with Aly1-GFP (pUG35-Aly1) or Aly2-GFP (pUG35-Aly2) in BY4742 cells was monitored using fluorescence microscopy at 2 and 8 min after endocytosis. Representative colocalizations at 8 min. are shown (white arrows). Quantification of colocalizing Aly-GFP foci with FM4-64 is shown at right. Scale bar, 5 μm. (B) Colocalization (white arrows) of Aly1-mCherry (p34Aly1-mCh) and Aly2-mCherry (p34Aly2-mCh) with Tlg1-GFP (p416-GFP-Tlg1) or Tlg2-GFP (pRS315-GFP-Tgl2) was assessed using fluorescence microscopy. Scale bar, 5 μm. (C) SNF7-mRFP cells expressing Aly1-GFP (pUG35-Aly1) and Aly2-GFP (pUG35-Aly2) were assessed for colocalization (white arrows) using fluorescence microscopy. Scale bar, 5 μm.

rescue *npr1*Δ growth on citrulline (Figure 6B) or increase the AzC sensitivity of *npr1*Δ cells (Figure 6C). In addition, Gap1 levels (Figure 6E) and Gap1 activity (Figure 6D) were only modestly increased when *Aly2* was overexpressed in comparison to *npr1*Δ cells containing the vector control. There was no significant change in Gap1 localization in *Aly2* overexpressing cells compared with the vector in *npr1*Δ (Figure 6F). Together, these findings show that regulation of Gap1 trafficking by Aly1 is independent of Npr1, whereas Aly2 acts primarily through an Npr1-dependent mechanism.

To determine if Aly1 or Aly2 are Npr1 substrates, we examined their electrophoretic mobility in *npr1*Δ cells. The electrophoretic mobility of Aly1 is identical in extracts of *npr1*Δ and wild-type cells (Figure 6G). In contrast, the electrophoretic mobility of Aly2 was increased in extracts of *npr1*Δ cells relative to wild-type cells, and this difference was abolished by phosphatase treatment (Figure 6G), suggesting Npr1-dependent phosphorylation of Aly2. To examine direct phosphorylation by Npr1, S-tagged Aly2 or S-tag control protein was purified from *E. coli* and incubated in vitro with purified Npr1 in the presence of ^{32}P-γ-ATP (Annan *et al.*, 2008). Npr1 phosphorylated Aly2 but not the S-tag alone, with a twofold increase in Aly2 phospho-signal in the presence of Npr1 compared with mock treatment, whereas the S-tag control phospho-signal is unchanged (Figure 6H). Thus, Aly2 serves as an Npr1 substrate in vitro. In this in vitro assay, the electrophoretic mobility of Aly2 does not change after phosphorylation by Npr1, perhaps because some phosphorylation sites are accessible only when Aly2 is bound to cargo and other intracellular regulators. Alternatively, the shift observed in wild-type versus *npr1*Δ extracts may be a combined result of direct phosphorylation and Npr1-dependent regulation of additional kinases/phosphatases that act on Aly2. Regardless, taken together, these in vivo and in vitro findings strongly suggest that the phosphorylation state and activity of Aly2 are directly regulated by Npr1 (see Figure 9).

Figure 6 (cont). SDS-PAGE and imaged on a Typhoon scanner for ^{32}P quantification or stained for total protein. pET-Aly2 phosphorylation ± Npr1 is shown (left-hand portion of panel). The mean fold-increase in phospho-signal upon addition of Npr1 kinase (normalized for loading) is plotted from three replicate experiments ± SDM for both pET-Aly2 and the pET tag alone (the latter is not phosphorylated by Npr1) in the right-hand portion of the panel.

Aly1 and Aly2 Localize to Endosomes

To determine where Aly1 and Aly2 reside within the cell, we examined colocalization of functional Aly1 and Aly2 GFP or RFP fusions with fluorescently tagged trafficking markers. Both Aly1 and Aly2 exhibited diffuse cytoplasmic fluorescence and localized to multiple intracellular foci (Figure 7A), as expected for soluble proteins that associate with membrane compartments. Aly1 and Aly2 colocalized with FM4-64–stained structures at 2 min (marks early endosomes/TGN) and 8 min (marks late endosomes/MVB) after dye internalization (Vida and Emr, 1995; Lewis *et al.*, 2000; Foote and Nothwehr, 2006; Figure 7A). Thus a significant portion of Aly1 and Aly2 localizes to endosomes. Aly1 and Aly2 also partially colocalized with Tlg1 and Tlg2 (Figure 7B), which are t-SNAREs that mediate fusion of vesicles trafficking between early endosomes and the TGN (Lewis *et al.*, 2000), indicating that Aly1 and Aly2 traffic between TGN/early endosomes. Finally, Aly1 and Aly2 colocalized partially with RFP-tagged Snf7, a component of the ESCRT III complex, indicating that some portion of Aly1 and Aly2 traffic to the MVB (Figure 7C). Reduced function of this Snf7-RFP has been noted and results in its accumulation in class E compartments (Huh *et al.*, 2003). Taken together, these results show that Aly1 and Aly2 partition between early and late endosomes.

Aly1 and Aly2 Colocalize and Interact with Clathrin

β-Arrestins interact directly with cargo proteins and the trafficking machinery, specifically clathrin and AP-2. MS analysis of Aly1- and Aly2-copurifying proteins identified clathrin heavy chain (Chc1) peptides (data not shown) and a subset of Aly1- and Aly2-foci colocalized with Chc1 (Figure 8A). This indicates that Aly1 and Aly2 associate with CCVs and may regulate clathrin-dependent trafficking.

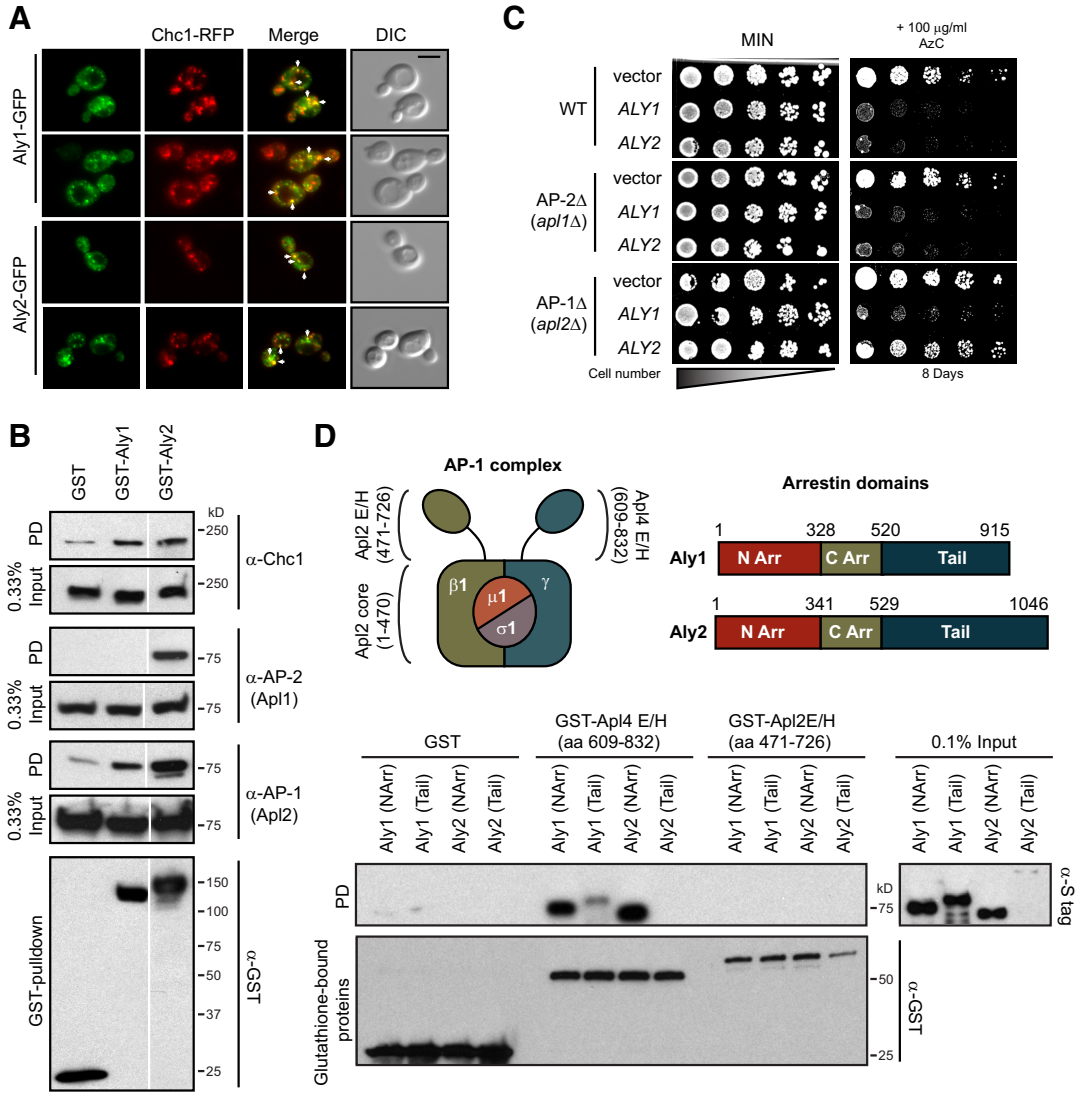

Figure 8. Aly1 and Aly2 colocalize with and copurify clathrin and adaptor complex subunits. (A) *CHC1*-mRFP cells expressing Aly1-GFP (pUG35-Aly1) and Aly2-GFP (pUG35-Aly2) were assessed for colocalization (white arrows) using fluorescence microscopy. Scale bar, 5 μm. (B) GST (pKK212), GST-Aly1 (pKK212-Aly1) or GST-Aly2 (pKK212-Aly2) were purified from extracts of BJ5459 cells with grown in SC-0.25% NH_4. Copurification of clathrin heavy chain (Chc1), the β-subunit of AP-1 (Apl2), and the β-subunit of AP-2 (Apl1) were assessed by WB (pulldown, PD). Samples were run on one gel, but line denotes lane removal. (C) Growth of WT (BY4741), *apl1*Δ (6802), or *apl2*Δ (4985) cells with pRS425, -Aly1, or -Aly2 on MIN-0.5% NH_4 ± AzC. (D) A schematic of illustrating the regions of the AP-1 complex and Aly1/Aly2 arrestins used in these in vitro binding studies is presented. GST, GST-Apl4 E/H (aa 609-832) and GST-Apl2 E/H (aa 471-726) were purified and binding of pET-Aly1-NArr (aa 1-328), pET-Aly1-Tail (aa 521-915), pET-Aly2-NArr (aa 1-341), or pET-Aly2-Tail (aa 530-1046) was assessed by WB (PD, pulldown).

Clathrin is recruited to nascent vesicles by AP complexes; AP-1 mediates TGN-endosome trafficking (Valdivia *et al.*, 2002; Waguri *et al.*, 2003), whereas AP-2 associates with endocytic CCVs (Bonifacino and Lippincott-Schwartz, 2003; Carroll *et al.*, 2009). MS analysis identified peptides from AP-1 subunits copurifying with Aly1 (data not shown), and a yeast proteomics study identified copurification of Aly2 with AP-2 subunits (Krogan *et al.*, 2006). We confirmed and extended these results; Chc1 and an AP-1 subunit (Apl2) were enriched significantly in purifications of both Aly1 and Aly2 compared with the GST control (Figure 8B) and an AP-2 subunit (Apl1) copurified with GST-Aly2 but not with GST or GST-Aly1 (Figure 8B). Aly1 and Aly2 association with AP-1 is consistent with Aly1 and Aly2 localization to endosomes and further supports an endosome-TGN trafficking function for these α-arrestins.

To determine if AP-1 or AP-2 are required for Aly1- or Aly2-dependent nutrient permease trafficking, *ALY1* or *ALY2* was overexpressed in cells lacking the β-subunit of AP-1 or AP-2 (Apl2 and Apl1, respectively; referred to here as *AP-1*Δ or *AP-2*Δ), and AzC sensitivity was monitored. Wild-type and *AP-2*Δ cells containing a vector grew similarly on AzC-medium (Figure 8C). However, *AP-1*Δ vector control cells were slightly resistant to AzC (Figure 8C), suggesting that AP-1 influences nutrient permease trafficking to the PM. *ALY1* overexpression increased the AzC sensitivity of wild-type, *AP-1*Δ, and *AP-2*Δ cells; thus Aly1 acts independently of AP-1 and AP-2 to increase amino acid

uptake at the cell surface. In contrast, overexpression of *ALY2* fails to increase AzC sensitivity in *AP-1*Δ cells (Figure 8C). These findings demonstrate a function for AP-1 in nutrient permease trafficking and establish that Aly2, but not Aly1, requires AP-1 to facilitate permease recycling from endosomes to the TGN and/or PM. In yeast AP-1 regulates endosome-TGN trafficking of Chs3 (chitin synthase III) (Valdivia *et al.*, 2002). Neither deletion nor overexpression of *ALY1* or *ALY2* altered Chs3 localization (Figure S3, A and B), indicating that Aly1 and Aly2 selectively modify the trafficking of AP-1-dependent cargo proteins.

We next examined direct interactions of Aly1 and Aly2 with the β- and γ-subunits of AP-1 (Apl2 and Apl4, respectively). We focused on Apl2 and Apl4 because they are structurally similar to the β-subunit of AP-2, which is the binding partner for mammalian β-arrestins (Laporte *et al.*, 1999). Apl2 and Apl4 are comprised of a ear/hinge domain (E/H), which interacts with clathrin and other trafficking factors (Yeung and Payne, 2001; Doray *et al.*, 2002; Duncan *et al.*, 2003), and a core domain, which interacts with other AP-1 proteins (Bonifacino and Lippincott-Schwartz, 2003). GST-fusions of the Apl2-Core, Apl2-E/H and Apl4-E/H were purified from *E. coli* and their binding to recombinant, S-tagged Aly1 and Aly2 domains assessed. Aly1 and Aly2 were divided into three regions: 1) the N-terminal arrestin-fold (NArr), 2) the C-terminal arrestin-fold (CArr), and 3) a C-terminal tail (Tail; Figure 8D; arrestin-domains based on Phyre structure predictions; Bennett-Lovsey *et al.*, 2008; Kelley and Sternberg, 2009). None of the arrestin constructs copurified with Apl2-Core (data not shown) or Apl2-E/H (Figure 8D). Importantly, both Aly1- and Aly2-NArr interacted strongly and specifically with Apl4-E/H (Figure 8D). A weaker interaction between the Aly1-Tail and Apl4-E/H was also observed (Figure 8D). Because the Aly2-Tail was expressed at extremely low levels in *E. coli*, its interaction with Apl4 E/H could not be determined (Figure 8D). Interactions of the Aly1- and Aly2-CArr could not be assessed as they copurified with GST-alone (data not shown). From these in vitro studies, we conclude that the NArr domains of Aly1 and Aly2 bind directly and specifically to the ear/hinge domain of Apl4, the γ-subunit of AP-1. Together our results provide evidence that the Aly2–AP-1 interaction is functionally important for Gap1 trafficking, and establish that, like β-arrestins, α-arrestins associate directly with clathrin-adaptor complexes.

DISCUSSION

In many cells, delivery of permeases to the PM is regulated by nutrients. For example, the Glut4 glucose transporter is sequestered in intracellular compartments and rapidly translocates to the PM to clear bloodstream glucose when muscle or adipose cells are exposed to insulin (Hou and Pessin, 2007). This clinically important response is compromised in type II diabetic patients. Similarly, in yeast grown on a preferred nitrogen source, Gap1 never reaches the PM, yet cells maintain ~3500 Gap1 molecules in intracellular pools (Roberg *et al.*, 1997b; von der Haar, 2008) so that Gap1 can be rapidly redistributed to the PM upon nitrogen starvation. The molecular mechanisms by which nutrients regulate such trafficking events are the subject of intense investigation. These studies demonstrate a novel role for arrestins as regulators of protein recycling and expand the repertoire of arrestin trafficking functions beyond their well-documented endocytic role. Furthermore, we provide the first evidence that, like β-arrestins, α-arrestins regulate trafficking by interacting directly with specific vesicle coat and signaling proteins, i.e., the clathrin adaptor AP-1 and Npr1 kinase.

Model of Aly1- and Aly2-mediated Trafficking

We propose that Aly1 and Aly2 promote Gap1 recycling from endosomes to the TGN and/or PM. Under nitrogen-replete conditions, Gap1 PM-activity is low as most of the permease is targeted to the vacuole for degradation. Under these conditions, Aly1 and Aly2 promote Gap1 recycling from endosomes, thereby increasing total Gap1 levels by rescuing some of the permease from vacuolar degradation (Figure 9). When nitrogen is limiting, Gap1 endosomal recycling is activated, causing a rapid increase in Gap1 activity at the PM; Aly1 and Aly2 are required to redistribute Gap1 under these conditions and act through distinct pathways with different proteins (Figure 9). Gap1 vesicles exiting endosomes may transit the TGN, which we favor for Aly2-mediated trafficking given its functional and physical interactions with AP-1, Lst4, and Npr1, or travel directly to the PM (Figure 9). Specific trafficking pathways regulated by Aly1 await identification. Our studies clearly demonstrate that endosomal recycling of Gap1 occurs via multiple routes, and establish Aly1 and Aly2 as tools that can be used to identify mechanisms governing nutrient-regulated Gap1 trafficking.

α-Arrestins Interact with Clathrin and Adaptins to Regulate Trafficking

β-Arrestins bind directly to clathrin and the β-subunit of AP-2 to package cargo proteins in endocytic vesicles (Goodman *et al.*, 1996; Laporte *et al.*, 1999). Similarly, Aly1 and Aly2 copurify with clathrin and an AP-1 subunit in vivo and interact directly with the γ-subunit of AP-1 in vitro. Aly1 and Aly2 may promote incorporation of Gap1 into clathrin- and AP-1–coated vesicles that transit from endosomes to the TGN, a trafficking interval in which clathrin/AP-1 operate (Valdivia *et al.*, 2002; Waguri *et al.*, 2003). In vivo, Aly2 requires AP-1 to affect Gap1 trafficking. In contrast, Aly1 altered Gap1 activity in cells lacking AP-1, thus Aly1 may regulate multiple classes of Gap1-containing vesicles. Aly2 (but not Aly1) interacts with the endocytic adaptor, AP-2 (Bonifacino and Lippincott-Schwartz, 2003; Carroll *et al.*, 2009). In addition to an endosomal recycling function, Aly2 may regulate endocytosis of other cargos.

We show that Aly1 and Aly2 interact directly with the γ-subunit of AP-1 (Apl4), which has not been previously reported for any arrestin. β-Arrestins bind to AP-2 through a conserved, C-terminal tail motif (Edeling *et al.*, 2006) that is not conserved in α-arrestins (Lin *et al.*, 2008). Although we find that the Aly1 C-terminal tail binds weakly to Apl4, there is a robust interaction between the N-terminal arrestin-domains of both Aly1 and Aly2 and the ear/hinge domain of Apl4. This identifies a novel mode of association with the trafficking machinery that may be conserved in other arrestins; β-arrestins required for vision also lack the conserved C-terminal tail motif responsible for AP-2 binding (Kiselev *et al.*, 2000).

α-Arrestins Associate with Signaling Proteins to Control Trafficking Decisions

Endocytosis of the yeast lysine permease, Lyp1, in response to excess ligand is regulated by the α-arrestin, Ldb19, whereas stress-induced endocytosis of Lyp1 is controlled by α-arrestin, Ecm21 (Lin *et al.*, 2008). Other α-arrestins also mediate cargo endocytosis selectively in response to specific environmental cues (Nikko and Pelham, 2009), suggesting

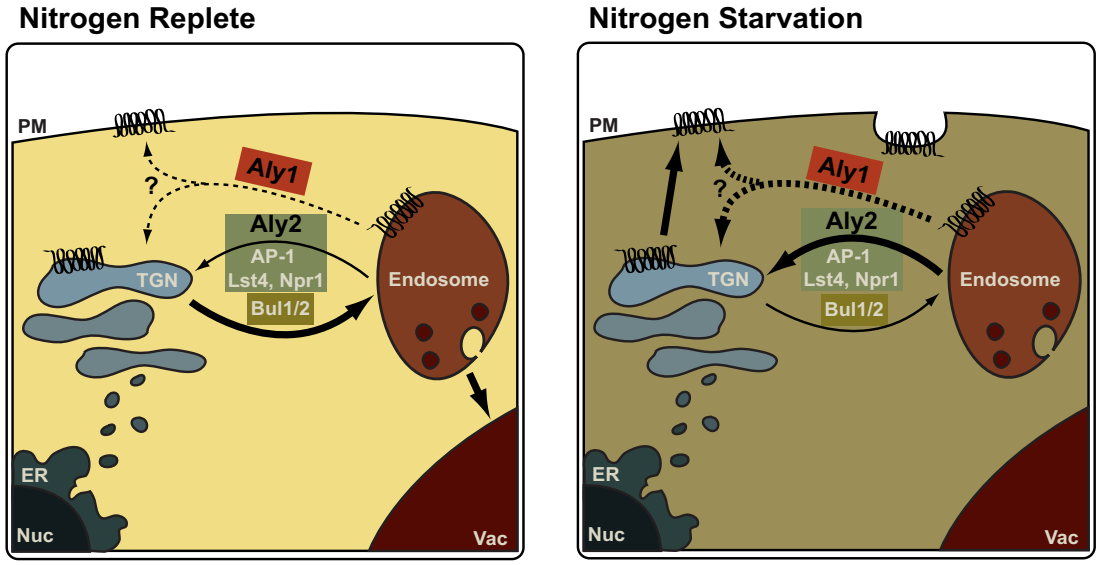

Figure 9. Model of Aly1- and Aly2-dependent, nutrient-regulated, Gap1 trafficking. Under nitrogen replete conditions, the majority of Gap1 is trafficked from the TGN to the endosome/vacuole without ever transiting the PM; Aly1/Aly2-dependent endosomal recycling of Gap1 is reduced, but contributes to overall Gap1 levels by diverting a portion of the permease from the endosome/vacuolar pathway. Npr1 is inactive. Under nitrogen starvation conditions, newly synthesized Gap1 transits from the TGN to PM, and Gap1 recycling from endosomal compartments is up-regulated. Npr1 is active. Aly1 and Aly2 mediate trafficking of Gap1 from endosomal compartments back to the TGN and/or the PM through two distinct pathways. Aly2 requires AP-1, Lst4, and Npr1 to mediate Gap1 recycling, and is proposed to operate in endosome-to-TGN trafficking based on the known activities of Lst4 and AP-1 in this interval. Aly1 functions independently of known recycling factors and may regulate Gap1 recycling from endosomes through multiple pathways that either go to the TGN and/or directly back to the PM. Black lines denote Gap1 trafficking paths, with thicker lines indicating the predominant trafficking pathways in that nutrient condition.

that signaling controls α-arrestin function; however, mechanisms underlying this regulation have not been identified.

Extracellular cues induce phosphorylation changes in β-arrestins that alter their trafficking and signaling activities (Shenoy and Lefkowitz, 2003). Similarly, we find that Aly2 interacts with and is directly phosphorylated by the nutrient-regulated kinase, Npr1. Nitrogen starvation activates Npr1 by relieving TORC1-inhibtion, and Npr1 is required for Gap1 translocation to the PM under these conditions (De Craene *et al.*, 2001). The mechanism by which Npr1 modifies Gap1 trafficking has been elusive; the only Npr1 substrate identified, Rho5, does not function in trafficking (Annan *et al.*, 2008). Our work is the first to identify a possible mechanism by which Npr1-dependent nutrient signaling impacts Gap1 distribution. Future studies will test the hypothesis that Npr1 positively regulates the ability of Aly2 to incorporate Gap1, and other Npr1-responsive permeases, into AP-1/clathrin coated vesicles (Schmidt *et al.*, 1998; Omura and Kodama, 2004; Boeckstaens *et al.*, 2007).

Regulation of Arrestins by Ubiquitination

Ubiquitination is a critical sorting determinant in protein trafficking. Nine of the 10 yeast α-arrestins, including Aly1 and Aly2, are ubiquitinated by the Rsp5 ubiquitin ligase (Kee *et al.*, 2006; Gupta *et al.*, 2007; Lin *et al.*, 2008). Aly1 and Aly2 mutants lacking Rsp5-binding sites are not ubiquitinated, and though present at increased levels, these mutant proteins fail to increase Gap1 levels at the PM (O'Donnell and Cyert, unpublished observations). Thus, Aly1 and Aly2 stability is Rsp5-dependent, as is Aly-mediated Gap1 trafficking. Rsp5 regulates key Gap1-trafficking decisions: Gap1 monoubiquitination at the PM stimulates endocytosis, whereas Gap1 polyubiquitination directs trafficking in the MVB (De Craene *et al.*, 2001; Helliwell *et al.*, 2001; Soetens *et al.*, 2001; Risinger and Kaiser, 2008). Ubiquitination is a dynamic modification, and ubiquitin chains are remodeled by addition and removal of ubiquitin as proteins transit the trafficking pathway; Rsp5 interacts with a deubiquitinating enzyme, Ubp2, which also influences protein trafficking (Kee *et al.*, 2006). Aly1 and Aly2 may serve as Rsp5-adaptors to regulate Gap1 ubiquitination in endosomal compartments and/or Rsp5-mediated ubiquitination of Aly1 and Aly2 may regulate their localization/function.

Expanded Trafficking Roles for Arrestins

We propose a new role for two α-arrestins as endocytosis-independent regulators of intracellular protein trafficking. The intracellular sorting we describe and arrestin-mediated endocytosis have functional similarities. We speculate that regulation of intracellular trafficking is a conserved arrestin function. In support of this idea, Vps26, a component of the retromer complex involved in endosome-to-TGN trafficking (Reddy and Seaman, 2001), is distantly related to α-arrestins and has a strikingly similar crystal structure to β-arrestins (Shi *et al.*, 2006). In addition to their endocytic role, β-arrestins regulate postendocytic endosome-to-PM recycling of membrane cargos. Finally, Bul1 and Bul2, Rsp5-adaptors involved in TGN-to-endosome sorting and endocytosis, are structurally related to arrestins (Nikko and Pelham, 2009). Thus, arrestin-fold domains provide a versatile architecture adaptable to many trafficking functions. As arrestin family members, Aly1 and Aly2 are ideally suited for the nutrient-dependent regulation of intracellular protein stores, which requires the convergence of signaling pathways with the protein trafficking machinery.

ACKNOWLEDGMENTS

We gratefully acknowledge materials received from Chris Kaiser (MIT), Gregory Payne (UCLA), and Bruno Andre (Free University of Brussels) and further thank Greg Payne for helpful discussions. We also thank W. James Nelson (Stanford), Adam Kwiatkowski, and Chris Toret for use of equipment and assistance with quantitative WB analysis and imaging. We also thank members of the Cyert lab, in particular Jagoree Roy and Kristen Jones Holmes, for their insights and critical reading of the manuscript. M.S.C and A.F.O. are supported by National Institutes of Health Grant GM-48728 and Agilent Technologies Foundation grants.

REFERENCES

Alvarez, C. E. (2008). On the origins of arrestin and rhodopsin. BMC Evol. Biol. *8*, 222.

Andreasson, C., Neve, E. P., and Ljungdahl, P. O. (2004). Four permeases import proline and the toxic proline analogue azetidine-2-carboxylate into yeast. Yeast *21*, 193–199.

Annan, R. B., Wu, C., Waller, D. D., Whiteway, M., and Thomas, D. Y. (2008). Rho5p is involved in mediating the osmotic stress response in *Saccharomyces cerevisiae*, and its activity is regulated via Msi1p and Npr1p by phosphorylation and ubiquitination. Eukaryot. Cell *7*, 1441–1449.

Ausubel, F. M. (1991). Current Protocols in Molecular Biology, New York: John Wiley & Sons.

Bennett-Lovsey, R. M., Herbert, A. D., Sternberg, M. J., and Kelley, L. A. (2008). Exploring the extremes of sequence/structure space with ensemble fold recognition in the program Phyre. Proteins *70*, 611–625.

Boeckstaens, M., Andre, B., and Marini, A. M. (2007). The yeast ammonium transport protein Mep2 and its positive regulator, the Npr1 kinase, play an important role in normal and pseudohyphal growth on various nitrogen media through retrieval of excreted ammonium. Mol. Microbiol. *64*, 534–546.

Bonifacino, J. S., and Lippincott-Schwartz, J. (2003). Coat proteins: shaping membrane transport. Nat. Rev. Mol. Cell Biol. *4*, 409–414.

Bultynck, G., Heath, V. L., Majeed, A. P., Galan, J. M., Haguenauer-Tsapis, R., and Cyert, M. S. (2006). Slm1 and slm2 are novel substrates of the calcineurin phosphatase required for heat stress-induced endocytosis of the yeast uracil permease. Mol. Cell. Biol. *26*, 4729–4745.

Carroll, S. Y., Stirling, P. C., Stimpson, H. E., Giesselmann, E., Schmitt, M. J., and Drubin, D. G. (2009). A yeast killer toxin screen provides insights into a/b toxin entry, trafficking, and killing mechanisms. Dev. Cell *17*, 552–560.

Chen, E. J., and Kaiser, C. A. (2002). Amino acids regulate the intracellular trafficking of the general amino acid permease of *Saccharomyces cerevisiae*. Proc. Natl. Acad. Sci. USA *99*, 14837–14842.

De Craene, J. O., Soetens, O., and Andre, B. (2001). The Npr1 kinase controls biosynthetic and endocytic sorting of the yeast Gap1 permease. J. Biol. Chem. *276*, 43939–43948.

Doray, B., Ghosh, P., Griffith, J., Geuze, H. J., and Kornfeld, S. (2002). Cooperation of GGAs and AP-1 in packaging MPRs at the trans-Golgi network. Science *297*, 1700–1703.

Duncan, M. C., Costaguta, G., and Payne, G. S. (2003). Yeast epsin-related proteins required for Golgi-endosome traffic define a gamma-adaptin ear-binding motif. Nat. Cell Biol. *5*, 77–81.

Edeling, M. A., Mishra, S. K., Keyel, P. A., Steinhauser, A. L., Collins, B. M., Roth, R., Heuser, J. E., Owen, D. J., and Traub, L. M. (2006). Molecular switches involving the AP-2 beta2 appendage regulate endocytic cargo selection and clathrin coat assembly. Dev. Cell *10*, 329–342.

Fernandez, G. E., and Payne, G. S. (2006). Laa1p, a conserved AP-1 accessory protein important for AP-1 localization in yeast. Mol. Biol. Cell *17*, 3304–3317.

Foote, C., and Nothwehr, S. F. (2006). The clathrin adaptor complex 1 directly binds to a sorting signal in Ste13p to reduce the rate of its trafficking to the late endosome of yeast. J. Cell Biol. *173*, 615–626.

Goldstein, A. L., and McCusker, J. H. (1999). Three new dominant drug resistance cassettes for gene disruption in *Saccharomyces cerevisiae*. Yeast *15*, 1541–1553.

Goodman, O. B., Jr., Krupnick, J. G., Santini, F., Gurevich, V. V., Penn, R. B., Gagnon, A. W., Keen, J. H., and Benovic, J. L. (1996). Beta-arrestin acts as a clathrin adaptor in endocytosis of the beta2-adrenergic receptor. Nature *383*, 447–450.

Grenson, M., Hou, C., and Crabeel, M. (1970). Multiplicity of the amino acid permeases in *Saccharomyces cerevisiae*. IV. Evidence for a general amino acid permease. J. Bacteriol. *103*, 770–777.

Grenson, M., Mousset, M., Wiame, J. M., and Bechet, J. (1966). Multiplicity of the amino acid permeases in *Saccharomyces cerevisiae*. I. Evidence for a specific arginine-transporting system. Biochim. Biophys. Acta *127*, 325–338.

Gupta, R., Kus, B., Fladd, C., Wasmuth, J., Tonikian, R., Sidhu, S., Krogan, N. J., Parkinson, J., and Rotin, D. (2007). Ubiquitination screen using protein microarrays for comprehensive identification of Rsp5 substrates in yeast. Mol. Syst. Biol. *3*, 116.

Hartwell, L. H. (1967). Macromolecule synthesis in temperature-sensitive mutants of yeast. J. Bacteriol. *93*, 1662–1670.

Helliwell, S. B., Losko, S., and Kaiser, C. A. (2001). Components of a ubiquitin ligase complex specify polyubiquitination and intracellular trafficking of the general amino acid permease. J. Cell Biol. *153*, 649–662.

Hou, J. C., and Pessin, J. E. (2007). Ins (endocytosis) and outs (exocytosis) of GLUT4 trafficking. Curr. Opin. Cell Biol. *19*, 466–473.

Huh, W. K., Falvo, J. V., Gerke, L. C., Carroll, A. S., Howson, R. W., Weissman, J. S., and O'Shea, E. K. (2003). Global analysis of protein localization in budding yeast. Nature *425*, 686–691.

Johnston, G. C., Pringle, J. R., and Hartwell, L. H. (1977). Coordination of growth with cell division in the yeast *Saccharomyces cerevisiae*. Exp. Cell Res. *105*, 79–98.

Kee, Y., Munoz, W., Lyon, N., and Huibregtse, J. M. (2006). The deubiquitinating enzyme Ubp2 modulates Rsp5-dependent Lys63-linked polyubiquitin conjugates in *Saccharomyces cerevisiae*. J. Biol. Chem. *281*, 36724–36731.

Kelley, L. A., and Sternberg, M. J. (2009). Protein structure prediction on the Web: a case study using the Phyre server. Nat. Protoc. *4*, 363–371.

Kiselev, A., Socolich, M., Vinos, J., Hardy, R. W., Zuker, C. S., and Ranganathan, R. (2000). A molecular pathway for light-dependent photoreceptor apoptosis in *Drosophila*. Neuron *28*, 139–152.

Krogan, N. J., *et al*. (2006). Global landscape of protein complexes in the yeast *Saccharomyces cerevisiae*. Nature *440*, 637–643.

Krupnick, J. G., and Benovic, J. L. (1998). The role of receptor kinases and arrestins in G protein-coupled receptor regulation. Annu. Rev. Pharmacol. Toxicol. *38*, 289–319.

Laporte, S. A., Oakley, R. H., Zhang, J., Holt, J. A., Ferguson, S. S., Caron, M. G., and Barak, L. S. (1999). The beta2-adrenergic receptor/betaarrestin complex recruits the clathrin adaptor AP-2 during endocytosis. Proc. Natl. Acad. Sci. USA *96*, 3712–3717.

Lauwers, E., Jacob, C., and Andre, B. (2009). K63-linked ubiquitin chains as a specific signal for protein sorting into the multivesicular body pathway. J. Cell Biol. *185*, 493–502.

Lewis, M. J., Nichols, B. J., Prescianotto-Baschong, C., Riezman, H., and Pelham, H. R. (2000). Specific retrieval of the exocytic SNARE Snc1p from early yeast endosomes. Mol. Biol. Cell *11*, 23–38.

Lin, C. H., MacGurn, J. A., Chu, T., Stefan, C. J., and Emr, S. D. (2008). Arrestin-related ubiquitin-ligase adaptors regulate endocytosis and protein turnover at the cell surface. Cell *135*, 714–725.

Longtine, M. S., McKenzie, A., 3rd, Demarini, D. J., Shah, N. G., Wach, A., Brachat, A., Philippsen, P., and Pringle, J. R. (1998). Additional modules for versatile and economical PCR-based gene deletion and modification in *Saccharomyces cerevisiae*. Yeast *14*, 953–961.

Nikko, E., Marini, A. M., and Andre, B. (2003). Permease recycling and ubiquitination status reveal a particular role for Bro1 in the multivesicular body pathway. J. Biol. Chem. *278*, 50732–50743.

Nikko, E., and Pelham, H. R. (2009). Arrestin-mediated endocytosis of yeast plasma membrane transporters. Traffic *10*, 1856–1867.

Nikko, E., Sullivan, J. A., and Pelham, H. R. (2008). Arrestin-like proteins mediate ubiquitination and endocytosis of the yeast metal transporter Smf1. EMBO Rep. *9*, 1216–1221.

Omura, F., and Kodama, Y. (2004). The N-terminal domain of yeast Bap2 permease is phosphorylated dependently on the Npr1 kinase in response to starvation. FEMS Microbiol. Lett. *230*, 227–234.

Raymond, C. K., Howald-Stevenson, I., Vater, C. A., and Stevens, T. H. (1992). Morphological classification of the yeast vacuolar protein sorting mutants: evidence for a prevacuolar compartment in class E vps mutants. Mol. Biol. Cell *3*, 1389–1402.

Reddy, J. V., and Seaman, M. N. (2001). Vps26p, a component of retromer, directs the interactions of Vps35p in endosome-to-Golgi retrieval. Mol. Biol. Cell *12*, 3242–3256.

Risinger, A. L., Cain, N. E., Chen, E. J., and Kaiser, C. A. (2006). Activity-dependent reversible inactivation of the general amino acid permease. Mol. Biol. Cell *17*, 4411–4419.

Risinger, A. L., and Kaiser, C. A. (2008). Different ubiquitin signals act at the Golgi and plasma membrane to direct GAP1 trafficking. Mol. Biol. Cell *19*, 2962–2972.

Roberg, K. J., Bickel, S., Rowley, N., and Kaiser, C. A. (1997a). Control of amino acid permease sorting in the late secretory pathway of *Saccharomyces cerevisiae* by SEC13, LST4, LST7 and LST8. Genetics *147*, 1569–1584.

Roberg, K. J., Rowley, N., and Kaiser, C. A. (1997b). Physiological regulation of membrane protein sorting late in the secretory pathway of *Saccharomyces cerevisiae*. J. Cell Biol. *137*, 1469–1482.

Rubio-Texeira, M., and Kaiser, C. A. (2006). Amino acids regulate retrieval of the yeast general amino acid permease from the vacuolar targeting pathway. Mol. Biol. Cell *17*, 3031–3050.

Schmidt, A., Beck, T., Koller, A., Kunz, J., and Hall, M. N. (1998). The TOR nutrient signalling pathway phosphorylates NPR1 and inhibits turnover of the tryptophan permease. EMBO J. *17*, 6924–6931.

Shenoy, S. K., and Lefkowitz, R. J. (2003). Multifaceted roles of beta-arrestins in the regulation of seven-membrane-spanning receptor trafficking and signalling. Biochem. J. *375*, 503–515.

Shenoy, S. K., McDonald, P. H., Kohout, T. A., and Lefkowitz, R. J. (2001). Regulation of receptor fate by ubiquitination of activated beta 2-adrenergic receptor and beta-arrestin. Science *294*, 1307–1313.

Shi, H., Rojas, R., Bonifacino, J. S., and Hurley, J. H. (2006). The retromer subunit Vps26 has an arrestin fold and binds Vps35 through its C-terminal domain. Nat. Struct. Mol. Biol. *13*, 540–548.

Soetens, O., De Craene, J. O., and Andre, B. (2001). Ubiquitin is required for sorting to the vacuole of the yeast general amino acid permease, Gap1. J. Biol. Chem. *276*, 43949–43957.

Soussi-Boudekou, S., and Andre, B. (1999). A co-activator of nitrogen-regulated transcription in *Saccharomyces cerevisiae*. Mol. Microbiol. *31*, 753–762.

Ungar, D., and Hughson, F. M. (2003). SNARE protein structure and function. Annu. Rev. Cell Dev. Biol. *19*, 493–517.

Urbanowski, J. L., and Piper, R. C. (1999). The iron transporter Fth1p forms a complex with the Fet5 iron oxidase and resides on the vacuolar membrane. J. Biol. Chem. *274*, 38061–38070.

Valdivia, R. H., Baggott, D., Chuang, J. S., and Schekman, R. W. (2002). The yeast clathrin adaptor protein complex 1 is required for the efficient retention of a subset of late Golgi membrane proteins. Dev. Cell *2*, 283–294.

Vida, T. A., and Emr, S. D. (1995). A new vital stain for visualizing vacuolar membrane dynamics and endocytosis in yeast. J. Cell Biol. *128*, 779–792.

Volland, C., Galan, J. M., Urban-Grimal, D., Devilliers, G., and Haguenauer-Tsapis, R. (1994). Endocytose and degradation of the uracil permease of *S. cerevisiae* under stress conditions: possible role of ubiquitin. Folia Microbiol. (Praha) *39*, 554–557.

von der Haar, T. (2008). A quantitative estimation of the global translational activity in logarithmically growing yeast cells. BMC Syst. Biol. *2*, 87.

Waguri, S., Dewitte, F., Le Borgne, R., Rouille, Y., Uchiyama, Y., Dubremetz, J. F., and Hoflack, B. (2003). Visualization of TGN to endosome trafficking through fluorescently labeled MPR and AP-1 in living cells. Mol. Biol. Cell *14*, 142–155.

Yeung, B. G., and Payne, G. S. (2001). Clathrin interactions with C-terminal regions of the yeast AP-1 beta and gamma subunits are important for AP-1 association with clathrin coats. Traffic *2*, 565–576.

Zheng, X. F., Florentino, D., Chen, J., Crabtree, G. R., and Schreiber, S. L. (1995). TOR kinase domains are required for two distinct functions, only one of which is inhibited by rapamycin. Cell *82*, 121–130.

Zhu, H., Bilgin, M., Bangham, R., Hall, D., Casamayor, A., Bertone, P., Lan, N., Jansen, R., Bidlingmaier, S., Houfek, T., Mitchell, T., Miller, P., Dean, R. A., Gerstein, M., and Snyder, M. (2001). Global analysis of protein activities using proteome chips. Science *293*, 2101–2105.